ACS NANO

www.acsnano.org

REVIEW

Recent Development of Implantable Chemical Sensors Utilizing Flexible and Biodegradable Materials for Biomedical Applications

Chen Hu,‖ Liu Wang,‖ Shangbin Liu,‖ Xing Sheng, and Lan Yin*

Cite This: *ACS Nano* 2024, 18, 3969−3995

Read Online

ACCESS | Metrics & More | Article Recommendations

ABSTRACT: Implantable chemical sensors built with flexible and biodegradable materials exhibit immense potential for seamless integration with biological systems by matching the mechanical properties of soft tissues and eliminating device retraction procedures. Compared with conventional hospital-based blood tests, implantable chemical sensors have the capability to achieve real-time monitoring with high accuracy of important biomarkers such as metabolites, neurotransmitters, and proteins, offering valuable insights for clinical applications. These innovative sensors could provide essential information for preventive diagnosis and effective intervention. To date, despite extensive research on flexible and bioresorbable materials for implantable electronics, the development of chemical sensors has faced several challenges related to materials and device design, resulting in only a limited number of successful accomplishments. This review highlights recent advancements in implantable chemical sensors based on flexible and biodegradable materials, encompassing their sensing strategies, materials strategies, and geometric configurations. The following discussions focus on demonstrated detection of various objects including ions, small molecules, and a few examples of macromolecules using flexible and/or bioresorbable implantable chemical sensors. Finally, we will present current challenges and explore potential future directions.

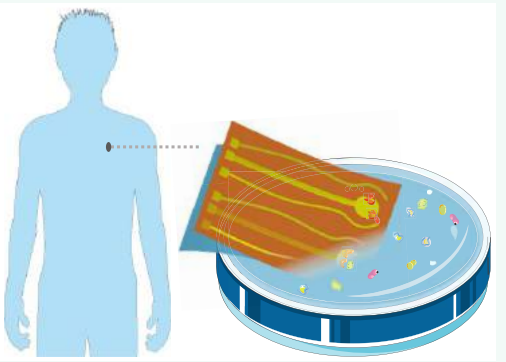

KEYWORDS: *implantable chemical sensors, flexible materials, biodegradable materials, sensing strategies, structural designs, ions, small molecules, macromolecules*

1. INTRODUCTION

Monitoring vital biomarkers in body fluids, such as sweat, urine, blood plasma, lymph, tears, cerebrospinal fluid, etc., is essential for assessing health status, diagnosing diseases, and adjusting postoperative interventions. Current methods for probing biomarkers often require frequent hospital visits and invasive procedures such as biopsies or blood draws.[1] These methods can reduce patient compliance and result in delayed information, which may lead to life-threatening situations in individuals with chronic diseases[2] (e.g., diabetes, kidney failure). Wearable chemical sensors offer a noninvasive method for the dynamic monitoring of analytes in body fluids such as sweat, granting users enhanced convenience and comfort. Nevertheless, the analytical accuracy of the data in correlation with specific disease states requires further validation. The development of implantable chemical sensors can potentially address these issues by offering real-time monitoring capabilities with high accuracy and extending clinical analysis to nonhospital settings. Generally, chemical sensing systems consist of bioreceptors to selectively interact with target analytes, transducers that convert receptor-analyte interaction into measurable signals, and analyzing systems for processing and recording data (Figure 1). These chemical sensors can be implanted inside human blood vessels, beneath the skin, or on the surface of organs to continuously probe local biomarkers. By detecting analytes with optimized selectivity, chemical sensors could offer unparalleled opportunities for real-time quantification of prognostic/diagnostic species, such as electrolytes (e.g., hydrogen ion (H^+), sodium ion (Na^+), potassium ion (K^+), calcium ion (Ca^{2+})),[3] blood gases (e.g., oxygen (O_2), carbon dioxide (CO_2)),[4,5] and metabolites (e.g., glucose, lactate).[6−8] For example, pH levels are important

Received: November 27, 2023
Revised: January 16, 2024
Accepted: January 18, 2024
Published: January 25, 2024

https://doi.org/10.1021/acsnano.3c11832
ACS Nano 2024, 18, 3969−3995

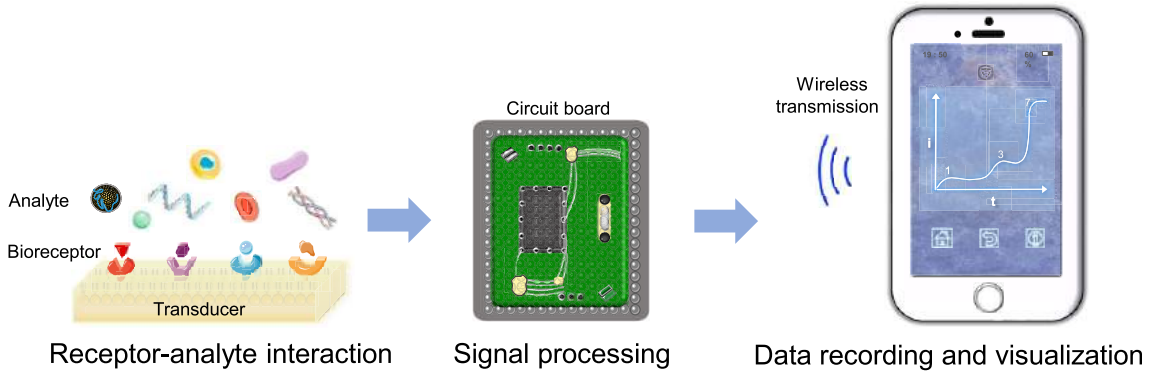

Figure 1. Schematic picture of chemical sensor working principle.

indicators of *in vivo* acid–base balance,[9] affecting enzymatic reactions,[10] tumor metastasis,[11] wound healing,[12] and cellular growth.[13] The continuous monitoring of pH in body fluids (e.g., saliva, urine, sweat) is essential for the early detection of conditions such as chronic periodontitis, kidney stones, and osteoporosis.[14] Na^+, K^+, Ca^{2+}, and various anions (e.g., chloride ion (Cl^-), bicarbonate ion (HCO^{3-})) are crucial in regulating the fluid dynamics and osmotic pressure of extracellular fluids. Real-time monitoring of these ions via implantable sensors could prevent neurological and organ damage, such as cognitive decline and cardiac arrhythmias, resulting from electrolyte imbalances.[15] O_2 and CO_2 are crucial biomarkers for energy metabolism in living organisms. Conditions like hypoxia and/or elevated CO_2 levels caused by hydrocephalus, brain tumors, and respiratory failure can lead to severe cellular and organ damage.[16] The prevalence of diabetes is reaching epidemic levels, giving rise to various complications like microangiopathy, atherosclerosis, coronary heart disease, peripheral vascular disease, peripheral vascular disease, and stroke. Implantable continuous glucose monitoring (CGM) devices[17] enable real-time adjustments to diabetes management by tracking glucose levels in both interstitial fluid and blood, facilitating recognition and treatment of associated symptoms. Elevated lactate levels may indicate acidosis, tissue hypoxia, sepsis, and organ failure.[18] In the fields of sports medicine and neurophysiology, the measurement of tissue lactate, often combined with glucose levels, serves as a crucial indicator of energy metabolism.[19] Examples of clinical applications include assisting patients in adjusting insulin doses and minimizing the risk of hyperglycemia by monitoring glucose concentrations,[20] diagnosing cancers by tracking pH levels,[21] and detecting colon cancer cells and pH values using a multifunctional endoscope-based interventional system.[22]

Despite significant advancements, there are still key challenges to be addressed in order for implantable chemical sensors to be effectively utilized in clinical settings and maximize their outcomes. First, conventional chemical sensors are often based on rigid and/or bulky materials, and the mechanical mismatch between the stiff components and soft human tissues could cause tissue damage and inflammation response,[23] and resulting fibrosis or accumulation of thrombus can easily degrade sensor performance.[24,25] In addition, most reported chemical sensors contain nondegradable components that could lead to materials retention in biological systems or require retraction procedures that would cause increased infection risks. In light of these challenges, the solution may lie in the realm of material science. Flexible and biodegradable materials that feature low modulus similar to soft tissues and benign degradation byproducts can provide many opportunities to incorporate sensing units, power supply, communication systems, and other components into chemical sensing systems that grant seamless integration with biological systems and collect accurate biological information without the need of secondary device retrieval surgery.[26] Moreover, biodegradable electronics are also attractive for green technologies. Materials that are biodegradable or derived from natural sources, combined with conductive polymers (CPs) and carbon-based conductive materials[27] have been employed to build eco-friendly sensors. Furthermore, the integration of transparent electrodes into electronic systems can maintain visual information when interfacing with complex physiological environments, enabling concurrent imaging analysis.[28] Research on innovative biomaterials,[29] manufacturing technologies,[30] and layout specification[31] yield implantable chemical sensors with potential capabilities in disease prevention, diagnosis, and treatment, which would otherwise be unattainable when employing traditional nondegradable and rigid sensors.

Focused on biomedical applications, this review highlights recent advances and accomplishments in implantable chemical sensors that integrate flexibility and/or biodegradability. The sensing strategies of implantable chemical sensors will be first discussed, followed by the summary of state-of-the-art advances in the structural design strategy to achieve flexible chemical sensors, including buckling/hierarchical buckling, origami, kirigami, porous structure, cracks, various two-dimensional (2D) shapes and "island-interconnection". In addition, biodegradable materials utilized to build implantable chemical sensors, including metals, semiconductors, dielectrics, natural and synthetic polymers will be reviewed. Finally, we showcase recent advancements in emerging implantable chemical sensors for various detection targets, including ions, small molecules, and larger organic macromolecules, demonstrating significant potential for biomedical applications. Challenges and outlooks of flexible and biodegradable chemical sensors for clinical medicine will be given at the end.

2. SENSING STRATEGIES OF IMPLANTABLE CHEMICAL SENSORS

Implantable chemical sensors have drawn great attention due to their ability to provide real-time and high-accuracy detection of biomarkers *in vivo*. Selecting a suitable sensing method is critical to achieving desirable performance for target applications, taking into account factors such as analyte type,

https://doi.org/10.1021/acsnano.3c11832
ACS Nano 2024, 18, 3969–3995

concentration, detection range, and selectivity. Electrochemical, mass-sensitive, and optical techniques are typically involved to achieve implantable chemical sensors. Their sensing characteristics, performance, and representative applications are summarized in Table 1.

2.1. Electrochemical Sensing Technique. By interacting with ions (e.g., Na^+, K^+, Ca^{2+}, H^+), small molecules (e.g., glucose, lactate, dopamine (DA), nitric oxide (NO)) and organic macromolecules (e.g., nucleic acids, proteins), electrochemical sensors convert chemical information into electrical signals (e.g., voltage (E), current (I), capacitance (C), and impedance (Z)) on conductive or semiconductive transducers. Electrochemical sensing offers several advantages, including high sensitivity, real-time monitoring capability, and easy integration into miniaturized and flexible systems.[41] Recognition elements (e.g., ion-selective membrane (ISM), enzyme, antibody, aptamer) are often immobilized on sensing electrodes to improve selectivity toward target analytes. Furthermore, detection limit and sensitivity can be optimized by decorating electrodes with various nanomaterials (e.g., graphene, fullerenes, magnetic nanomaterials, and metal nanoparticles),[42,43] by promoting the effective surface area and assisting electron transfer. Potentiometry, amperometry, voltammetry, impedance spectroscopy, and sensing based on field-effect transistor (FET) or organic electrochemical transistor (OECT) are representative electrochemical sensing techniques for implantable biosensors (Figure 2a).

2.1.1. Potentiometric Sensors. Potentiometric biosensors are typically adopted to detect ion concentrations in the physiological environment by measuring the potential difference between a working electrode (WE) and a reference electrode (RE)[44] (Figure 2a (I)). The WE is often decorated with an ISM to enhance sensing selectivity toward a particular type of ion, which is referred to as ion-selective electrodes (ISEs). Compared with other analytical methodologies, potentiometric sensors utilizing ISEs exhibit the distinct advantages of free maintenance, easy miniaturization, cost-effectiveness, and rapid response. Moreover, the associated near zero-current flow can minimize potential interference to surrounding tissues, which is particularly important when probing neuronal activity.[45] CPs such as polypyrrole (PPy), poly(3-octylthiophene) (POT), and poly(3,4-ethylenedioxythiophene) (PEDOT), in conjunction with various nanomaterials, have been extensively utilized to form conductive contacts beneath the ISMs, allowing a well-defined pathway for ion-to-electron transduction[46] (Figure 2a (I)). These nanomaterials can significantly augment the sensitivity of potentiometric sensors based on their excellent physical and chemical properties, such as large surface area-to-volume ratio, high charge transfer capacity, robust conductivity, and exceptional electrocatalytic activity. Wang et al.[47] have employed the potentiometric method to create a flexible DA sensor made of carbon nanotube (CNT) fiber electrodes in tandem with electrophysiology to monitor DA fluctuations in the brain, showing a low limit of detection (LOD) of 5 nM. Moreover, ISEs have been rationally designed and integrated with tailor-made stretchable materials, enabling continuous monitoring in physiological fluids and cells. For example, Tahirbegi et al.[48] have reported an endoscopic needle-shaped platform featuring a micro-ISE on a soft sensing microarray, enabling *in situ* examination of nitrate levels and pH.

2.1.2. Amperometric and Voltammetric Sensors. Amperometric measurement is widely used in implantable electro-

Table 1. Characteristics, Performance, and Representative Application of Different Sensing Techniques

sensor type	sensor characteristics	performance	challenges	representative applications
Electrochemical techniques				
Potentiometric	Tracking changes in voltage, current, impedance or capacitance that occur due to variations in the concentrations of analytes	Wide dynamic ranges, low LOD, good sensitivity, fast response	Enhancement of stability and sensitivity	Cerebral DA monitoring,[32] NO monitoring in the heart and joint cavity,[33] subcutaneous glucose monitoring,[34] and pH monitoring[35]
Amperometric				
Voltammetric				
EIS		Label-free detection, good sensitivity, and easy implementation	Improvement of time resolution, selectivity, and stability	
FET		Low LOD, high sensitivity, easy miniaturization	Improvement of stability for FET and liquid-gated FET, and response time for OECT	
Liquid-gated FET				
OECT				
Mass-sensitive techniques				
QCM	Detection of frequency shift in crystal oscillation caused by analytes binding	Fast response, high sensitivity, low cost, ease of use	Enhancement of selectivity	Blood glucose monitoring[36]
Optical techniques				
Fluorescence	Measurement of changes in absorption or emission	Wide dynamic ranges, good sensitivity, low LOD, simple integration	Improvement of sensitivity, stability, and system miniaturization	pH monitoring in the subcutis,[37] HE4 monitoring,[38] NO and H_2S in the gastrointestinal tract,[39] and cerebral Cu^{2+} monitoring[40]
Chemiluminescence				
ECL				
PEC	Tracking of photocurrent resulting from light absorption			

https://doi.org/10.1021/acsnano.3c11832
ACS Nano 2024, 18, 3969−3995

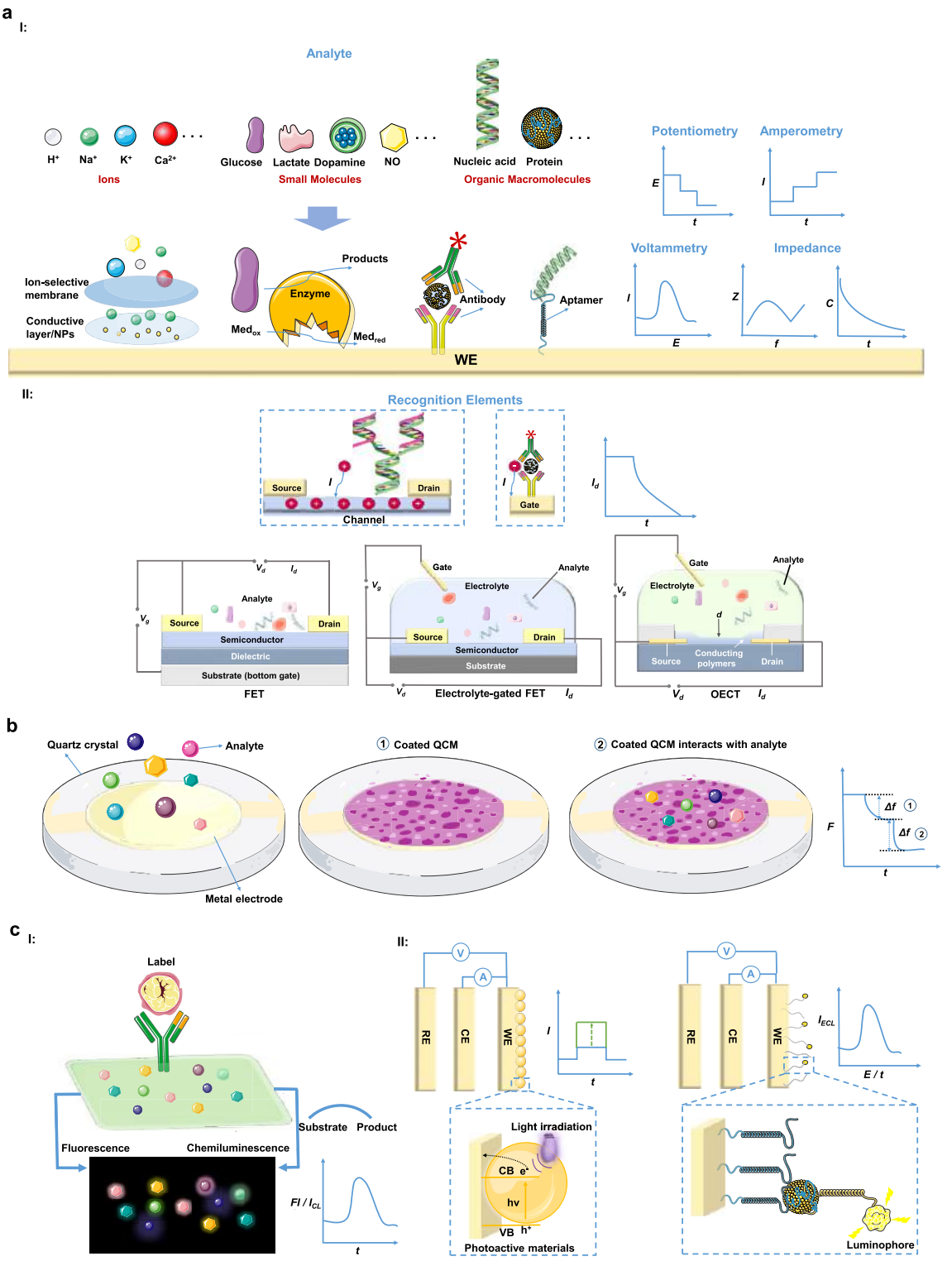

Figure 2. Sensing strategies of implantable chemical sensors. (a) (I) Electrochemical sensing of various analytes. Representative examples illustrate sensing ions using ion-selective electrode, sensing small molecules using enzyme electrode, and sensing organic macromolecules using antibody-modified and aptamer-modified electrodes. Electrochemical sensing methods include potentiometry, amperometry, voltammetry, and impedance spectroscopy. (II) Schematic illustrations of FET sensor with bottom-gate top-contact configurations, liquid-gated FET sensors, and OECT sensors. (b) Typical structure of quartz crystal microbalance (QCM) sensor and the illustration of frequency decreasing due to the interaction of target analytes with active layer coating. (c) Schematic illustrations of optical-based sensors commonly adopted for *in vivo* chemical sensing. (I) Schematic illustrations of fluorescence-based and chemiluminescence-based sensors. (II) Left: Illustration of the photoelectrochemical (PEC) sensor consisting of a three-electrode system and an external light source; Right: Illustration of the electrochemiluminescence (ECL) sensor composed of a three-electrode system and aptamers with luminescent groups. WE, working electrode; CE, counter electrode; RE, reference electrode; I_d, drain current; V_d, drain voltage; V_g, gate voltage; VB, valence band; CB, conduction band.

https://doi.org/10.1021/acsnano.3c11832
ACS Nano 2024, 18, 3969−3995

chemical sensors for probing metabolites (e.g., small molecules such as glucose and lactate), and it is typically performed using a three-electrode system, which includes a WE made of noble metals (e.g., gold (Au), platinum (Pt)) or low-cost carbon-based materials (e.g., glassy carbon, carbon paste, CNT) for analyte recognition, a counter electrode (CE) made of inert conducting material (e.g., Pt, graphite) to ensure current flow, and a RE (e.g., silver/silver chloride (Ag/AgCl)). A constant potential is applied between the WE and RE to promote a redox reaction and the corresponding current between the WE and CE is measured. A target-specific enzyme (e.g., glucose oxidase (GOx), lactic dehydrogenase (LDH), and acetaminase) is often incorporated on the electrode to catalyze redox reactions to ensure selective detection of target molecules[49] (Figure 2a (I)). For instance, Vashist[50] has highlighted the utilization of needle-type enzymatic amperometric biosensors in building commercial CGM systems and the correlation of recorded currents and subcutaneous glucose concentration can be established. Furthermore, the introduction of nanomaterials on electrodes can enhance sensitivity and reduce detection limits by facilitating electron transfer.[51] For example, Pu et al.[52] have developed an innovative implantable enzyme-based amperometric biosensor, incorporating a cylindrical WE with three-dimensional (3D) nanostructures composed of graphene and Pt nanoparticles, facilitating a low LOD of glucose at 3.54 mg/dL. Nanostructured materials can also stabilize enzyme activity or directly replace natural enzymes (i.e., artificial nanoenzymes). For example, by electroless plating of nickel and Au layers onto 3D porous laser-induced graphene (LIG) electrodes, a flexible nonenzymatic glucose sensor has been fabricated by Zhu et al.,[53] exhibiting stable electrochemical signals after being bent back-and-forth 500 times and immersed in phosphate-buffered saline (PBS) containing 0.1 mM NaCl for 30 days.

Voltammetry shares similarities with amperometry, but it differs in that the applied voltage is not constant and can be employed in various modes, including cyclic voltammetry, differential pulse voltammetry, adsorptive stripping voltammetry, square wave voltammetry, etc. Voltammetry is often used to investigate electroactive molecules through oxidation or reduction reactions around a specific potential. For example, Choi et al.[54] have utilized fast-scan cyclic voltammetry to detect neurotransmitters such as serotonin (5-HT), DA, and norepinephrine (NP) at low voltages, offering significant insights into neurotransmission and pharmacology. Furthermore, organic macromolecules such as proteins and nucleic acids can also be detected by voltammetry through affinity recognition which is triggered by the interaction of analyte with recognition biomolecules (e.g., antibodies, aptamers, ribonucleic acid (RNA), and deoxyribonucleic acid (DNA)).[55] It is worth mentioning that different types of voltammetry have their advantages and can be adapted to various application scenarios. For instance, differential pulse voltammetry and square wave voltammetry can minimize capacitive current and enable improved sensitivity,[56] and stripping voltammetry is capable of detecting trace levels of heavy metals in physiological environments.[57,58]

2.1.3. Electrochemical Impedance Spectroscopy (EIS) Sensors. EIS sensors are engineered to acquire highly accurate information by measuring the impedance or capacitance of bioaffinity reactions, without the formation of degradative products at the interfaces[59] (Figure 2a (I)). Impedance is typically determined by applying a small sinusoidal voltage disturbance in conjunction with a redox pair that can undergo a redox reaction. Slight fluctuations in analyte concentration within body fluids can block or facilitate the electron transfer leading to the change of the impedance. However, for *in vivo* chronic application, introducing a redox pair into the body for detection purposes is not feasible. As a result, an alternative approach, nonfaradaic impedance spectroscopy (NIS), is being explored.[60] This method conceptualizes the electrode/electrolyte interface as a parallel-plate capacitor, the capacitance can be calculated by eq 1,

$$C = \frac{\varepsilon \varepsilon_0 A}{d} \tag{1}$$

where C represents the capacitance, ε represents the dielectric constant, ε_0 is the permittivity of free space, A denotes the area of the parallel plate, and d is the distance separating the two plates. When analytes adhere to the electrode surface, C diminishes due to a decrease of ε and an increase of d. Hence, the reduction in C can serve as a highly sensitive indicator of binding events.

Numerous implanted EIS sensors have been applied in various areas of clinical diagnostics[61] such as quantitative investigations of single-cell,[62,63] cancerous tissue characterization,[64,65] and virus (or bacteria) detection.[66,67] Nguyen et al.[68] have reported a millimeter-scale tripolar EIS biosensor combined with biopsy tools for use in endoscopy to discriminate colorectal tumors by sensing tissue impedance. The EIS device implanted in mice bearing the CT-26 colon tumor line showed the ability to detect tumors in diseased tissue with good sensitivity and specificity. Nanostructured materials and bioactive compounds have also been introduced to enhance EIS signals and detection sensitivity.[69] Specifically, Gao et al.[70] have designed a modern EIS-based DNA sensor featuring Au@bismuth sulfide (Bi_2S_3) core−shell nanorods modified electrodes to identify DNA in the concentration range of 10 fmol/L to 1 nmol/L. Nevertheless, EIS is ultrasensitive to biofouling and it remains a challenge to achieve fast scan in the wide frequency band.[71]

2.1.4. FET and OECT Sensors. The aforementioned electrochemical sensors are primarily based on conductive electrodes, whereas biosensors leverage the advantages of semiconductive components and can achieve significantly improved sensitivity. FET sensors have therefore received significant attention due to their ultrasensitivity, rapid response, compact size, cost-effectiveness, and ease of integration. Furthermore, FET biosensors are characterized by a low drain voltage (V_d), typically below 0.3 V, which results in negligible damage to biological systems. A metal-oxide-semiconductor field-effect transistor (MOSFET) represents the common structure of FET-based biosensors. As shown in Figure 2a (II), FET in a bottom-gate top-contact configuration can directly use the substrate as the gate, and the oxide layer as the dielectric, avoiding the damage to channel materials during complex fabrication processes which is often involved in top-gate FET.[72] Upon the application of a low gate potential (V_g), electrons accumulate in the top region of the channel materials, forming a conductive channel and allowing conduction between the drain and source. At this juncture, the binding of analytes (e.g., gases, ions, organics, and biomolecules) with receptor elements fixed on the channel materials induces a change in the channel's current, and thus associated concentration of analytes can be quantified.[73,74] As a crucial component of FET sensors, channel materials have

https://doi.org/10.1021/acsnano.3c11832
ACS Nano 2024, 18, 3969−3995

been extensively explored for a wide array of materials, such as silicon (Si),[75] molybdenum disulfide (MoS_2),[76] graphene,[77] and CNTs.[78] FET devices can be fabricated at the micro or nano level while retaining desirable sensitivity.[79] For instance, Zhou et al.[80] have reported the preparation of needle-type FET microsensors modified with aptamer/reduced graphene oxide (RGO). Thanks to their high sensitivity and selectivity, excellent mechanical toughness, and minimal damage to biological systems, the device has been successfully utilized to monitor real-time DA activity in the brains of rodents. Tian et al.[81] have developed a 3D-kinked nanoscale FET to insert into a single cell to record changes in pH and action potential.

Liquid-gated FET (or electrolyte-gated FET) is another common type of FET-based biosensor (Figure 2a (II)), which is similar to MOSFET but it differs in that the gate electrode is separated from the channel and placed in the analyte solutions.[82] The application of gate voltage (V_g) causes ions to drift in the electrolyte, leading to the accumulation of charges at the gate−electrolyte and channel-electrolyte interface, thus modulating the channel current (I_d). When recognition elements are modified on the surface of gate electrodes or channels, associated reactions or binding of target biomolecules in the electrolyte can change the conductivity of the channel, subsequently altering the drain current. The interaction of ions at the subnanometer scale can result in strong electrostatic effects at the interfaces, allowing for low operation voltages to be achieved in liquid-gated FET. Furthermore, compared to traditional FET, the gate electrodes in liquid-gated FET can be positioned coplanar to the source and drain electrodes, simplifying the fabrication procedure.[83] Chen et al.[84] have demonstrated the use of liquid-gated FET sensors for the detection of charged biomolecules through electronic responses generated by specific interactions between DNA and CNTs.

OECT represents an alternative technique for *in vivo* detection of crucial biomarkers, owing to their facile processing, exceptional sensitivity, and outstanding biocompatibility and flexibility.[85] The conductivity of the channel is modulated by the gate voltage through an electrochemical reaction that controls the injection of ions from the electrolyte into the channel, leading to a change in its doping state[86] (Figure 2a (II)). Unlike conventional FET where charge influence is limited to the surface regions, the doping process occurs throughout the entire volume of the OECT channel, which enables large modulation of channel current under low gate voltages, thereby significantly enhancing the sensitivity and efficiency.[87] Gate electrodes or channels of OECT can also be modified with recognition elements to improve sensing selectivity.

2.2. Quartz Crystal Microbalance (QCM) Sensors. As the most prevalent devices in mass-sensitive sensors, QCM sensors hold significant application potential in the healthcare field. The key advantages of QCM sensors include label-free detection, rapid response, high sensitivity, robust stability, and excellent repeatability. By applying voltage, the natural piezoelectric quartz crystals in QCM sensors can oscillate at a specific frequency (F). The frequency is designated as the output signal which is associated with the mass (m) coated on the active quartz surface[88] according to the Sauerbrey equation:

$$\Delta f = -\frac{2f_0^2}{A\sqrt{\rho_q \mu_q}}\Delta m \tag{2}$$

where Δf represents the resonant frequency shift of QCM, f_0 is the baseline resonant frequency, Δm signifies the mass alteration, A denotes the electrode surface area, μ_q, and ρ_q are the shear modulus and density of quartz crystal, respectively.[89] As depicted in Figure 2b, recognition elements are often coated onto the QCM electrode to identify target analytes through the adsorption−desorption mechanism. This coating process results in a decrease in the QCM resonant frequency. Subsequently, the adsorption of analyte molecules onto the coated QCM surface leads to a further reduction in frequency. Hence, the analyte concentration and the QCM's frequency can be concurrently tracked using a high-precision frequency meter. For instance, Dou et al.[36] have designed QCM sensors for real-time detection of blood glucose concentration (BGC) by modifying quartz crystals with boronic acid-containing hydrogels using a surface-initiated polymerization method. These QCM sensors demonstrated rapid response and an extensive monitoring range in the subcutaneous tissue of rats, outperforming existing boronic acid (H_3BO_3)-hydrogel systems.

2.3. Optical Chemical Sensors. Optical-based biosensors have emerged as a robust tool in probing biomarkers, owing to their contactless characteristics, high sensitivity, less interference, and excellent signal-to-noise ratio.[90] Fluorescence-based and chemiluminescence-based optical sensors, photoelectrochemical (PEC) sensors, and electrochemiluminescence (ECL) sensors are commonly adopted for *in vivo* chemical sensing.

2.3.1. Fluorescence-Based and Chemiluminescence-Based Sensors. Fluorescence-based sensors determine the concentration of analytes primarily through variations in the intensity of fluorescence-containing optical-sensing molecules that absorb energy from a light source and re-emit at a longer wavelength.[91] Direct fluorescence biosensor is commonly used for biosensing, which contains a specific ligand tagged with a fluorescent label (Figure 2c (I)) that selectively interacts with the target analyte, yielding a fluorescence intensity (FI) proportional to the analyte's concentration.[92] For instance, Rzhechitskiy et al.[93] have engineered fluorescent pH sensors embedded within the adipose fin, employing SNARF-1 as a well-characterized pH-sensitive molecular probe. SNARF-1 exhibits pH-dependent alteration in its fluorescence emission spectrum from yellow-orange to deep red. The solution pH can therefore be associated with the intensity ratio between these two wavelengths.

Chemiluminescence is an optical radiation phenomenon in which photons are triggered by chemical redox reactions due to the returns of a molecule to the ground state after the excitation to the singlet excited state.[94] External excitation light sources are therefore not required. The analyte concentration can directly influence the reaction rate and chemiluminescence intensity (I_{CL}). Inda-Webb et al.[39] have reported a miniaturized device that integrated a chemiluminescence detector with bacterial chambers for monitoring NO and hydrogen sulfide (H_2S) in the gastrointestinal tract. Biosensing bacteria housed within chambers detect these metabolites with a high luminescence output. The information is wirelessly transmitted in real-time from inside the body of the living pig to an external recording device.

https://doi.org/10.1021/acsnano.3c11832
ACS Nano 2024, 18, 3969−3995

2.3.2. PEC Sensors. Photoactive materials are essential components in the PEC detection process,[95,96] as they can absorb light photons and generate electrons excited from the valence band (VB) to conduction band (CB), forming photogenerated carriers (electron−hole pairs) to produce photocurrents in photoelectrochemical reactions[97,98] (Figure 2c (II)). Under illuminated conditions, when the interaction between target molecules and photoactive materials occurs at the PEC sensor surface, there is a corresponding change in the photocurrent signal. The intimate correlation between analyte concentration and variations in the photocurrent signal enables PEC sensors to achieve precise identification and quantitative analysis of targets. Thus far, great progress has been achieved in the development of nanostructured materials exhibiting outstanding PEC properties, encompassing organic semiconductor materials,[99,100] inorganic semiconductor materials,[101,102] and semiconductor-based heterojunctions.[103−106] Particularly, biocompatible nanomaterials with enhanced photoelectric conversion efficiency are frequently selected for modifying the electrode/solution interface in implantable PEC sensors.[107] Combining the advantages of optical and electrochemical sensors, PEC sensors inherit attributes such as fast response, cost-effectiveness, and miniaturization.[108] Moreover, the separation of the excitation source (light source) and detection signal (electrical signal) results in reduced background noise[109] and enhanced sensitivity compared to other biochemical sensors (e.g., fluorescence-based sensors, surface plasmon resonance sensors, surface-enhanced Raman scattering techniques, electrochemical sensors). PEC sensors utilizing noncontact light stimuli[110] present significant promise for sophisticated detection of *in vivo* molecules, including ions, disease-related DNA,[111] microRNA (miRNA),[112] antigens,[113] aptamers,[114] protein markers,[115] and circulating tumor cells.[116] Tao et al.[40] have utilized electrodes constructed with an Au film infused with cadmium sulfide@zinc oxide (CdS@ZnO) photoactive material to fabricate an implantable optical fiber (OF)-based PEC microsensor. The sensor can selectively monitor variations in extracellular copper ion (Cu^{2+}) levels, a direct marker of cerebral ischemia/reperfusion and related neurological disorders, in three different brain regions of living rats.

2.3.3. ECL Sensors. ECL sensors are based on the chemiluminescence phenomenon, where electrogenerated luminous species generated during a redox reaction undergo electron transfer processes, leading to the formation of electronically excited states that emit light.[117,118] Analogous to PEC sensors, ECL sensors also function using a three-electrode system, in which the WE is modified with the recognition biomolecules to serve as the biosensing electrode (Figure 2c (II)). For example, aptamers can be labeled with luminescent groups and immobilized on the electrode surface. The aptamer molecules may dissociate or be released from the electrodes, resulting in alterations to the electrochemical luminescence intensity (I_{ECL}). A linear relationship between ECL intensity and concentration of the analyte enables quantitative detection. The elimination of excitation lasers and optical filters allows for negligible background noise and a simplified detection apparatus in ECL sensors. In addition, due to the precise control over the light emission position, ECL sensors exhibit enhanced selectivity, high simplicity, and excellent reproducibility, manifesting itself as a powerful analytical method with high precision for the ultrasensitive detection of markers related to disease-resistance trait[119] in body fluids. Nonetheless, ECL sensors are less frequently employed for long-term monitoring due to the substantial deterioration of assay sensitivity and specificity during the contamination process, which is induced by the nonspecific binding of interfering substances.[120] To address this issue, Cao et al.[121] have proposed a robust antifouling ECL sensing interface to detect exosomes in real-time by combining bioreceptors with zwitteronic chemistries on a biocompatible ECL transducer composed of protonated graphitic carbon nitride ($g\text{-}C_3N_4$) and titanium carbide ($Ti_3C_2T_x$) MXene nanosheets. This work offers a practical strategy for designing implantable ECL biosensors in biological fluids.

3. FLEXIBLE AND BIODEGRADABLE MATERIALS FOR IMPLANTABLE CHEMICAL SENSORS

Flexible materials play a key role in building implantable chemical sensors with enhanced biocompatibility and desirable mechanical properties mimicking soft and dynamic tissues. Specifically, flexible characteristics are crucial for achieving conformal attachment to curvilinear biological surfaces and tolerating dynamic deformation, which enables the capture of high-quality biosignals.[122] Combining flexible materials with thin-film or nanowire form factors and structural design can realize mechanical modulus comparable to that of biotissues, minimizing immune response and potential tissue damage.[123] Biodegradable materials endow devices with degradable characteristics that eliminate materials residues after monitoring windows and avoid retrieval surgeries. This biodegradability is particularly advantageous for temporary implants used in regenerative medicine and postsurgical monitoring. Fibrotic encapsulation often occurs around implanted devices, and their removal can lead to secondary tissue damage or even life-threatening lacerations. The use of biodegradable materials can potentially resolve these issues, avoiding the retention of permanent materials and reducing associated infection risks.[124] In the following, we will review common material strategies employed to achieve flexible and/or biodegradable chemical sensors.

3.1. Flexible Materials for Implantable Chemical Sensors. Implantable chemical sensors with soft properties mimicking biological tissues are essential for minimizing mechanical irritation and immune response. Using inherently soft materials such as elastomers, hydrogels, and liquid metals[125] as building blocks represents the most intuitive approach for developing soft implantable sensors. Alternatively, fabricating traditionally rigid electronic materials such as metals, dielectrics, and semiconductors[126] in the thin film, fiber or nanowire format enables sufficient flexibility while also leveraging established manufacturing technologies.[127,128] When used in conjunction with various structural designs, soft and stretchable characteristics can be further accomplished by these flexible materials, facilitating seamless integration with living organisms.[129] Here, we highlight strategies and considerations in various structural designs, including buckling structures, origami and kirigami, porous and crack-based structures, diverse 2D-shaped configurations, and the "island-bridge" structure.[130] In general, porous and 2D shape-based structures have demonstrated applications in implantable chemical sensing. Meanwhile, other structures are mainly applied in wearable chemical sensors and their utilization in implantable chemical sensors warrants further exploration. These approaches enable devices to maintain excellent

https://doi.org/10.1021/acsnano.3c11832
ACS Nano 2024, 18, 3969−3995

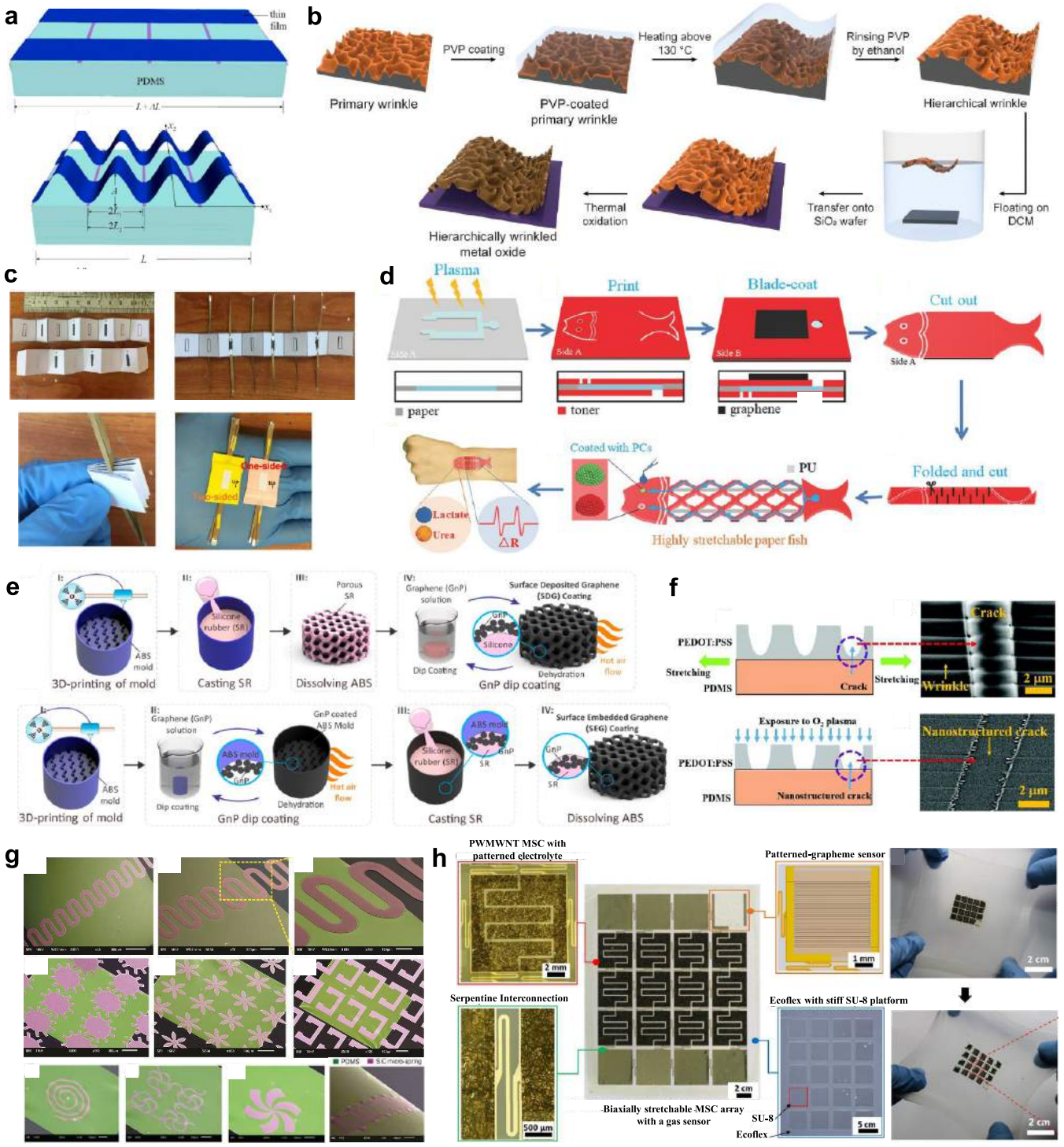

Figure 3. Structural designs of flexible electronic materials. (a) Schematic illustration of the fabrication process of the wavy Si (GaAs) nanoribbons on the PDMS substrate. Reprinted with permission from ref [135]. Copyright 2007 American Institute of Physics. (b) Schematic illustration of the fabrication process of the CuO films with hierarchical buckled structure on the SiO_2 wafer. Reprinted with permission from ref [136]. Copyright 2019 American Chemical Society. (c) Images depicting the design of P/G ink-based origami hierarchical sensors array (OHSA) with six-channel configuration on a folding paper. Reprinted with permission under a Creative Commons CC BY License from ref [139]. Copyright 2019 Nature Publishing Group. (d) Schematic illustration of the fabrication process of the bioinspired kirigami fish sensor. Reprinted with permission from ref [141]. Copyright 2018 Wiley-VCH. (e) Schematic representation of the fabrication processes of porous surface-deposited graphene (SDG) and surface-embedded graphene (SEG) sensors. Reprinted with permission from ref [147]. Copyright 2020 American Chemical Society. (f) Cross-sectional illustration and surface morphology of a PEDOT:PSS thin film exhibiting nanostructured cracks. Reprinted with permission from ref [154]. Copyright 2019 Royal Society of Chemistry. (g) SEM images of various microstructures on the sacrificial aluminum layer, including serpentine, gear, flower, "U" shape, spiral, and propeller shapes. Reprinted with permission from ref [160]. Copyright 2020 Wiley-VCH. (h) Biaxially stretchable patterned-graphene sensor integrated with a PWMWNT MSC array and its optical image before and after 40% biaxial stretching. Reprinted with permission from ref [166]. Copyright 2015 Elsevier.

https://doi.org/10.1021/acsnano.3c11832
ACS Nano 2024, 18, 3969−3995

performance even when subjected to deformation in physiological environments.[131,132]

3.1.1. Buckling Structure. Shaping high-modulus materials into buckled (wavy/wrinkled) films or stripes is an effective strategy for electronic materials. When subjected to external stress, thin films with buckled structures unfold to minimize potential mechanical damage by reducing their buckling amplitude and increasing wavelength. For example, Bowden et al.[133] have attached titanium (Ti) and Au films to thermally pre-expanded polydimethylsiloxane (PDMS) elastomeric substrates, inducing compressive stress and wave patterns in the metal films upon subsequent cooling. Sun et al.[134,135] have fabricated gallium arsenide (GaAs) and Si nanoribbons with controlled buckling patterns that can also be integrated into PDMS through the casting and curing of elastomers (Figure 3a). As a type of buckled configuration, hierarchical buckled structures offer superior mechanical characteristics, enhanced electrical conductivity, and increased sensitivity and selectivity for sensors. For instance, Jung et al.[136] have developed a hierarchical cupric oxide (CuO) wrinkle structure using a polyvinylpyrrolidone (PVP) sacrificial layer and integrated it into acetone gas-sensing devices (Figure 3b). These devices exhibited considerable improvements in both response time and sensitivity.

3.1.2. Origami and Kirigami. Through origami techniques, a planar sensor sheet can be effectively transformed into a complex and collapsible 3D structure,[137] creating a repeating pattern of alternating mountain and valley folds on the device sheet.[138] As illustrated in Figure 3c, Zhang et al.[139] have fabricated an origami-based hierarchical sensor array using conductive ink. The sensor demonstrated specific sensing abilities to physical and chemical stimuli, including temperature, light, air pressure, relative humidity, and volatile organic compounds. Kirigami techniques, stemming from origami, combine paper cutting and folding methods, and can be effectively utilized to achieve stretchable devices.[140] For instance, Gao et al.[141] have designed a fish-scale-like wearable biosensor with high stretchability and excellent adaptability for detecting lactate, urea, and uric acid in sweat samples (Figure 3d). Won et al.[142] have achieved transparent electrodes by combining ultrathin and flexible silver nanowires/colorless-polyimide (AgNWs/cPI) composites with laser-patterned kirigami structures. These kirigami-engineered patterns enhanced the elasticity and stretchability of electrodes, making them suitable for E-skin applications.

3.1.3. Porous and Cracks Structure. A variety of materials with porous structures exhibit volumetric alterations when exposed to external stress, demonstrating good scalability and stretchability attributes. These characteristics have been effectively leveraged in flexible sensors, either as substrates or as functional components. Metals or metal oxides,[143,144] Si,[145] and carbon-based materials[146] (e.g., graphene, CNTs) have been fabricated with porous structures, and play critical roles in wearable chemical sensors due to their high surface area and desirable piezoresistive properties. For instance, Davoodi et al.[147] have reported a graphene-doped porous silicone-based sensor with exceptional flexibility and strain-recoverability, capable of monitoring humidity, temperature, and human motion. The device incorporated two distinct coating processes, namely surface-deposited graphene (SDG) and surface-embedded graphene (SEG) with sacrificial acrylonitrile-butadiene-styrene (ABS) molds (Figure 3e). Metal–organic frameworks (MOFs)[148] represent alternative porous materials with potential applications in implantable chemical sensing.[149] Ling et al.[150] have presented a three-electrode system incorporating two-dimensional (copper metal–organic framework) Cu-MOF layers for ascorbic acid (AA), hydrogen peroxide (H_2O_2), and L-histidine (L-His) detection. The same group[151] has also engineered multichannel implantable flexible sensors based on highly porous Cu-MOF and cobalt metal–organic framework (Co-MOF) materials, and continuous *in vivo* detection of L-tryptophan in blood and interstitial fluids was demonstrated. In addition, the introduction of nanocracks in chemical sensors has been reported to enhance resistance ratio, electrical charge transport properties, and sensitivity.[152,153] For instance, Sarkar et al.[154] have developed a flexible conducting polymer film with quasi-periodic cracks for ultrasensitive vapor sensing. Figure 3f illustrates the nanostructured crack by removing the residual poly(3,4-ethylenedioxythiophene) (PEDOT):poly(styrenesulfonate) (PSS) in the crack region using O_2 plasma. The electron percolation path was partly turned due to the swelling-mediated linkage of the residual polymer in the crack.

3.1.4. Various 2D Shapes. Diverse 2D shapes have been implemented to achieve flexible and conductive components. For example, spring-shaped stretchable electrodes composed of Au wires were integrated into the PDMS matrix utilizing standard lithography techniques.[155] These 2D structured electrodes demonstrated superior stretchability compared to traditional straight counterparts. A variety of conducting materials, such as metal,[156] silver halide,[157] and carbon-based substances,[158,159] have been fabricated into various 2D structures to construct flexible and stretchable chemical sensors. Pham et al.[160] have developed an innovative fabrication technique for transferring silicon carbide (SiC) microstructures with diverse 2D morphologies (e.g., serpentine, gear, flower, "U" shape, spiral, and propeller) onto PDMS substrates using sacrificial layers (Figure 3g). These adaptable semiconductor patterns possessed the potential to impart flexibility and stretchability to a wide range of implantable sensors, delivering physiological signals and real-time feedback for disease management. Bai et al.[161] have successfully devised a Si-based bioresorbable photonic platform for detecting biochemical species such as glucose. Specifically, by incorporating monocrystalline-Si filaments with zigzag or spiral structures onto polylacticcoglycolic acid (PLGA) substrates, the device demonstrated enhanced extension capabilities and adjustable degradation performance. By incorporating a U-shaped Si waveguide with a PLGA film, the biosensor exhibited real-time *in vivo* monitoring of blood oxygenation through transmission spectroscopy in rodents. The 2D structure of implantable sensors enables seamless integration with subcutaneous tissue, minimizing mechanical irritation and enhancing interface reliability.

3.1.5. Island-Bridge Structure. Chemical sensors utilizing an island-bridge architecture can maintain their electrical properties even when subjected to large external strain. This is primarily due to the segregated functional components strategically positioned on relatively "rigid" islands within the sensor system.[162] In juxtaposition, the "soft" conductive bridges, adopting 3D and 2D morphologies such as wavy,[163] serpentine,[164] and fractal structures,[165] can deform intra-plane and extra-plane under the influence of applied strain, endowing these devices with superior flexibility and stretchability. Yun et al.[166] have developed a flexible patterned-graphene nitrogen dioxide (NO_2) gas sensor, powered by an all-solid-state

https://doi.org/10.1021/acsnano.3c11832
ACS Nano 2024, 18, 3969–3995

Table 2. Summary of Representative Biodegradable Materials Utilized in Biodegradable Electronics with a Focus on Chemical Sensors, Highlighting Their Dissolution Behavior and Representative Applications

biodegradable material	test conditions	dissolution rates	components in representative sensors	representative biodegradable applications
Metals				
Mg	Hank's solution, RT	4.8 μm/h[183]	Interconnects	Cerebral DA monitoring[32]
Mo	Hank's solution, 37 °C	0.2−0.6 nm/h[184]	Interconnects	NO monitoring in the heart and joint cavity[33]
Fe	Hank's solution, RT	7−9 μm/h[184]	Electrodes	Cerebral DA monitoring[32]
W	Hank's solution, 37 °C	0.2−0.8 nm/h[184]	Electrodes	Subcutaneous glucose monitoring[34]
Zn	Hank's solution, RT	0.3 μm/h[183]	Electrodes	Subcutaneous glucose monitoring[34]
Semiconductors				
Si	PBS, 37 °C	4.1 nm/day[185]	Semiconductor	Cerebral pH monitoring[186]
Ge	PBS, 37 °C	3.1 nm/day[185]	Electrodes	Strain and temperature monitoring[187]
ZnO	PBS, 37 °C	4 nm/h[183]	Semiconductor	LEDs[188]
Oxides and nitrides				
SiO_2	PBS, 37 °C	0.1 nm/day[189]	Membranes	Subcutaneous pH monitoring[190]
Si_3N_4	PBS, 37 °C	0.794 nm/day[189]	Encapsulation	Intracranial pressure monitoring[191]
Polymers				
PLGA	PBS, 37 °C	Total degradation in 8 h[192]	Substrate	NO_x gas monitoring[192]
POC	PBS, RT, pH 10	Total degradation in several weeks[35]	Substrate	pH monitoring[35]
PCL	PBS, 37 °C, pH 11	Total degradation in 15 h[32]	Substrate	Cerebral DA monitoring[32]
Silk fibroin	Protease XIV solution, 37 °C	75% mass loss in 10 days[193]	Substrate	Subcutaneous O_2 monitoring[193]

microsupercapacitor (MSC) array, composed of polyaniline-wrapped multiwalled carbon nanotubes (PMWNTs) (Figure 3h). A rigid SU-8 platform, introduced between the serpentine Au bridges and the deformable Ecoflex substrate, initiated a modulus gradient and mitigated the strain concentration at the island-bridge boundaries, ensuring electrochemical stability. Liquid metal can be harnessed to connect an array of nine microsupercapacitors (MSCs) and a gas sensor based on a hybrid film of multiwalled carbon nanotubes/stannic oxide (MWNT/SnO_2) for monitoring applications.[167] This wearable chemical sensor exhibited consistent current and resistance responses to NO_2 concentrations of 200 ppm, even under a tensile strain of 50%.

In addition to flexibility, stretchability is crucial for implantable sensors to withstand tissue tension in highly mobile body regions. Various strategies to increase the stretchability have been suggested. Structural designs such as serpentine or buckling structures have been widely used to improve the stretchability of inorganic electronic materials.[162] Molecular engineering serves as an effective method to enhance the stretchability of polymer materials. For example, the design of a topological supramolecular network enables highly conductive and stretchable bioelectronic devices.[168] Moreover, nanowires[169] and liquid metals[170] that are stretchable in single or aggregated forms have been developed to achieve stretchability and flexibility in sensors. For instance, Choi et al.[171] have created a 3D porous metal-based electrode using Ag−Au core−shell nanowire foam (AACNF) with low density, high electrical conductivity, and mechanical stability, suitable for advanced energy devices and biohybrid electrodes. Kim et al.[172] have introduced a substrate-less nanomesh artificial skin sensor capable of measuring finger movements from multiple joints. Hong et al.[173] have designed Cu nanowire network electrodes with an encapsulation structure for skin-mountable flexible, stretchable, and wearable electronics. Won et al.[174] have validated the safety of liquid metal embedded elastomers (LMEEs) containing eutectic gallium−indium (EGaIn) liquid metal embedded in a soft rubber matrix, demonstrating their suitability for use in implantable biomedical sensors. Kim et al.[175] have presented a room-temperature, stretchable, sticker-like soldering process utilizing a patternable free-standing liquid AgNW composite thin film. A temperature/humidity sensor module based on this composite has been realized with dimensions compact enough for mounting on a fingernail.

3.2. Biodegradable Materials for Implantable Chemical Sensors. A variety of biodegradable electronic materials have been proposed to achieve implantable chemical sensors, including interconnects, dielectric layers, semiconducting components, encapsulation, substrate, and sophisticated data acquisition systems.[176] When exposed to body fluids, these constituent materials undergo either physical or chemical dissolution, including hydrolysis,[177] enzymolysis,[178] oxidation,[179] and disintegration,[180] producing nontoxic metabolizable byproducts, thereby avoiding any potential harm to tissues at the implantation site.[181] Specifically, proposed dissolvable materials encompass metals (e.g., magnesium (Mg), zinc (Zn), molybdenum (Mo), iron (Fe), and tungsten (W)), semiconductors (e.g., Si, germanium (Ge), ZnO), dielectrics (e.g., silicon oxides (SiO_2), silicon nitrides (Si_3N_4)), and natural and synthetic polymers (e.g., gelatin, collagen, cellulose, chitosan, PLGA, polycaprolactone (PCL), poly(caprolactone)-poly(glycerol sebacate) (PCL−PGS), poly(vinyl alcohol) (PVA), poly(L-lactide) (PLLA), poly(1,8-octanediol-*co*-citrate) (POC), etc.).[182] These materials have been used in biodegradable electronics, and Mg, Zn, Mo, W, Fe, Si, SiO_2, PLGA, POC, PCL and silk fibroin have demonstrated applications in biodegradable chemical sensors, as summarized in Table 2. The following section will examine the degradation characteristics of these materials.

3.2.1. Metals. Biodegradable metals, including Mg, Zn, Mo, Fe, and W are widely adopted as electrodes and interconnects in implantable chemical sensors due to their desirable electrical conductivity, excellent biocompatibility, and ease of fabrica-

https://doi.org/10.1021/acsnano.3c11832
ACS Nano 2024, 18, 3969−3995

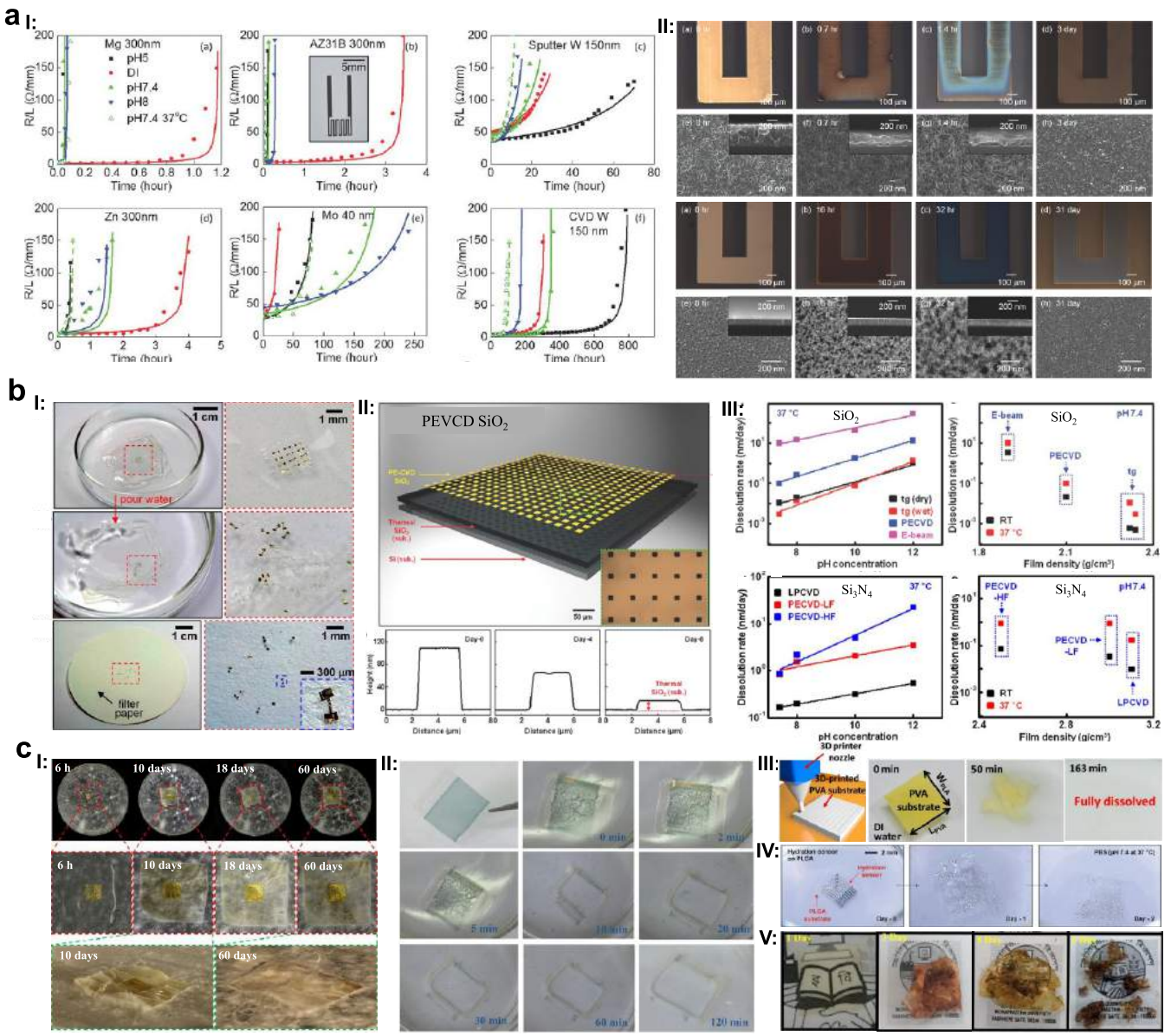

Figure 4. Dissolution behavior of biodegradable materials. (a) Evolution of microstructure and electronic performance associated with the dissolution of various metals. (I) Resistance change of Mg, Mg alloy, Zn, Mo, and W thin film as a function of time during dissolution in simulated biofluids or DI water, modulated by pH and temperature; (II) Optical and SEM images revealing microstructural changes in Mg and W during dissolution in DI water. Reprinted with permission from ref [184]. Copyright 2013 Wiley-VCH. (b) Dissolution behavior of semiconductors and insulators. (I) Images of the dissolution of Si devices on silk substrates, at different time intervals (left) with magnified views (right). Reprinted with permission from ref [202]. Copyright 2009 American Institute of Physics. (II) Schematic illustration and measured thickness change of SiO_2 dissolution in buffer solutions at 37 °C. (III) Dissolution rate of silicon nitride and silicon oxide films at varied densities in buffer solutions under different pH and temperature. Reprinted with permission from ref [189]. Copyright 2014 Wiley-VCH. (c) Dissolution of polymers at different stages. (I) Photographs of the cellulose nanofibril (CNF) during the degradation process (top) with magnified views (middle) and tilted views (bottom) after initiating the degradation process. Reprinted with permission under a Creative Commons CC BY License from ref [214]. Copyright 2015 Nature Publishing Group. (II) Images depicting the chronological progression of fibroin substrate dissolution in deionized (DI) water under ambient conditions. Reprinted with permission from ref [215]. Copyright 2016 Wiley-VCH. (III) The 3D-printed PVA substrate and its image showing the time sequence of the degradation in DI water. Reprinted with permission from ref [219]. Copyright 2018 American Chemical Society. (IV) Images of a transient hydration sensor on a PLGA film at various stages of dissolution during immersion in PBS at 37 °C. Reprinted with permission from ref [217]. Copyright 2014 Wiley-VCH. (V) Images depicting the degradation stages of a chitosan/PVP (CHP) substrate in soil. Reprinted with permission from ref [220]. Copyright 2019 American Chemical Society.

tion.[194] Yin et al.[184] have studied the electrical degradation rates and associated changes in the microstructure of these metals in deionized (DI) water (Figure 4a (I) and (II)). Degradation mechanisms of Mg in DI water or biofluids can be presented as follows:[195]

$$Mg + 2H_2O \rightarrow Mg(OH)_2 \downarrow + H_2\uparrow \quad (3)$$

Magnesium (Mg) and its alloys exhibit relatively fast degradation rates, necessitating the use of an encapsulation layer to protect the Mg film. As degradation progresses, the

https://doi.org/10.1021/acsnano.3c11832
ACS Nano 2024, 18, 3969−3995

metal surface becomes rougher, leading to needle-like structures composed of magnesium oxide (MgO) and magnesium hydroxide ($Mg(OH)_2$) that can subsequently be dissolved and eliminated through processes of homeostasis and fluid circulation.[196] In a flexible and bioresorbable electrochemical sensor, Mg (~200 nm) has been adopted as electrical contacts and interconnects that are encapsulated by SiO_2, enabling continuous, real-time dopamine monitoring.[32]

In comparison to Mg, Zn shares a similar degradation mechanism (as presented in eq 4) but exhibits a slower degradation rate in solution. The electrical dissolution rate of Mg is determined to be 4.8 μm/h in Hank's solution at room temperature (RT), while the degradation rate for Zn is 0.3 μm/h.[183]

$$Zn + 2H_2O \rightarrow Zn(OH)_2 \downarrow + H_2\uparrow \quad (4)$$

Transition metals, notably Mo and W, demonstrate relatively slow dissolution rates, making them promising candidates for building implantable devices that can ensure sufficient operational time frames in physiological environments.[197] Studies showed that Mo and W thin films exhibit electrical dissolution rates of 0.2−0.6 nm/h and 0.2−0.8 nm/h respectively in Hank's solution (pH between 5 and 8) (Figure 4a (I)).[184] Corresponding degradation is presented in eqs 5 and 6, respectively.[183]

$$2Mo + 2H_2O + 3O_2 \rightarrow 2H_2MoO_4 \quad (5)$$

$$2W + 2H_2O + 3O_2 \rightarrow 2H_2WO_4 \quad (6)$$

Zn, W, and Mo are commonly used as electrodes in implantable biodegradable chemical sensors. For example, a fully printed, bioresorbable glucose sensor with a Zn WE, a Mo CE, and a Mo−W RE has been developed for subcutaneous glucose monitoring.[34]

Fe has been utilized as the sensing or catalytic component in implantable chemical sensors.[32,198] The electrical dissolution rate of Fe is determined to be 7−9 μm/h in Hank's solution at RT.[184] The degradation chemistry, as depicted in eq 7,[183] involves the oxidation of ferrous ion (Fe^{2+}) in an oxygen environment, leading to the formation of hydroxides that dissolve slowly afterward.

$$4Fe + 3O_2 + 6H_2O \rightarrow 4Fe(OH)_3\downarrow \quad (7)$$

3.2.2. Semiconductors. Semiconductors such as Si, Ge, and ZnO thin films are dissolvable in biofluids. The degradation products of Si and Ge are ortho-silicic acid ($Si(OH)_4$) and germanic acid (H_2GeO_3) respectively (eq 8 and 9). The dissolution of ZnO is shown in eq 10.

$$Si + 4H_2O \rightarrow Si(OH)_4 + 2H_2\uparrow \quad (8)$$

$$Ge + O_2 + H_2O \rightarrow H_2GeO_3 \quad (9)$$

$$ZnO + H_2O \rightarrow Zn(OH)\downarrow \quad (10)$$

Degradation rates of silicon nanomembranes (Si NMs) are affected by many factors, including doping species, doping levels, temperature, pH, solution ions, surface charges, sample size, etc.[199,200] For example, elevated temperature and high concentrations of chlorides and phosphates can substantially enhance Si dissolution, presumably via a nucleophilic dissolution mechanism. In addition, the introduction of Ca^{2+}, magnesium ions (Mg^{2+}), and bovine serum have also been demonstrated to accelerate dissolution rates. Degradation rates of various types of Si, including single crystal Si, polycrystalline silicon (polySi), and amorphous silicon (a-Si) have been comprehensively summarized in a previous review.[201] Si NMs and silicon nanoribbons (Si NRs) are commonly used as the active components of implantable chemical sensors, which demonstrate the detection of various chemicals such as DA.[32] As depicted in Figure 4b (I), Kim et al.[202] have developed an implantable, bioresorbable device utilizing Si NMs, leveraging strategies to integrate single-crystalline Si with flexible silk substrates. The dissolution rate of Si NMs and Ge has been determined to be 4.1 nm/day and 3.1 nm/day in PBS at 37 °C, respectively.[185] The increase in temperature and pH can also significantly increase the dissolution rate of Ge, and the dissolution of silicon germanium (SiGe) exhibits a strongly accelerated rate in bovine serum. Ge has been used as the sensing component in strain and temperature sensors.[187] ZnO grown on monocrystalline Si (111) by pulsed laser deposition (PLD) shows a dissolution rate of 4 nm/h in PBS at pH 7.4 and 37 °C.[183] ZnO has been used as semiconducting materials in transient light-emitting diodes (LEDs).[188]

3.2.3. Insulators. Insulators such as nitrides, oxides, and polymers can serve as dielectrics, substrates, or encapsulations for implantable devices.[203] The dissolution rates of these insulating materials are typically low and are influenced by many factors such as porosity and density.

3.2.3.1. Oxides Dielectrics. In implantable and bioresorbable sensors, SiO_2[204] and Si_3N_4 often serve as the encapsulation layer because of their slow degradation. These oxides can also serve as the dielectric layers and membranes in pH sensors.[37,190,205] The hydrolysis of SiO_2 and Si_3N_4 is extensively researched[206,207] and their dissolution in biofluids are presented as follows:

$$SiO_2 + 2H_2O \rightarrow Si(OH)_3 \quad (11)$$

$$Si_3N_4 + 6H_2O \rightarrow 3SiO_2 + 4NH_3\uparrow \quad (12)$$

$$Si_3N_4 + 12H_2O \rightarrow 3Si(OH)_4 + 4NH_3\uparrow \quad (13)$$

Studies show that SiO_2 and Si_3N_4 deposited by plasma-enhanced chemical vapor deposition (PEVCD) exhibit electrical dissolution rates of 0.1 nm/day and 0.794 nm/day respectively in buffer solutions (in pH 7.4) at 37 °C.[189] The degradation rates are greatly affected by pH, deposition conditions, and the presence of specific ions (e.g., K^+, Na^+, Ca^{2+}, and Mg^{2+}).[208] As shown in Figure 4b (II) and (III), Kang et al.[189] have found that the dissolution rates of SiO_2 deposited via electron-beam (e-beam) evaporation and PEVCD exhibit much faster kinetics compared to that of thermally grown SiO_2. Additionally, Si_3N_4 fabricated through low-pressure chemical vapor deposition (LPCVD) presents slower degradation compared to those fabricated by PECVD.

3.2.3.2. Polymers. Given their ease of production, flexible mechanical properties, and adjustable degradation rates, biodegradable polymers often serve as dielectric or encapsulation layers for implantable devices.[209] These polymers undergo degradation through enzymatic breakdown, hydrolysis, oxidation, or photooxidation,[210] targeting specific vulnerable sites in the polymer chain backbone. Natural polymers, such as cellulose, silk, fibroin, gelatin, collagen, chitosan, alginate, dextran, starch, and others,[211−213] possess inherent bioactivity, due to similarities with biological macromolecules. For example, Jung et al.[214] and Wang et al.[215] have utilized completely soluble cellulose nanofibril and

https://doi.org/10.1021/acsnano.3c11832
ACS Nano 2024, 18, 3969−3995

Table 3. Analytes, Sensing Strategies, Performance, and Stability of Implantable Chemical Sensors

analytes	sensing strategies	performance	detection time frame	ref
Ions				
K^+, Na^+, Ca^{2+}	Potentiometry	Flexible sensors, good sensitivity (64.7, 82.1, 34.8 mV/dec for K^+, Na^+, Ca^{2+} respectively)	2 weeks	228
K^+, Na^+, Ca^{2+}	Potentiometry	Flexible sensors, good sensitivity (48.38, 52.28, 28.86 mV/mM for K^+, Na^+, Ca^{2+} respectively), good reproducibility	2 weeks	229
H^+	FET	Stretchable and biodegradable sensors, good sensitivity (0.1−4 μS/pH), wide range (pH 3−10)	5 days	35
H^+	Fluorescence	Flexible and bioresorbable sensors, good sensitivity (6.2 mV/pH), media range (pH 4−7.5), good reproducibility	220 h	37
Small molecules				
DA, NP, 5-HT, EP	Voltammetry	Flexible and stretchable sensors, low LOD (5.6, 7.2, 3.5, 6.6 nM for DA, NP, 5-HT, EP respectively), wide range (10 nM to 1 μM)	16 weeks	230
DA	OECT	Flexible sensors, Low LOD (1 nM), wide range (30 nM to 0.1 mM)		231
DA	Amperometry	Flexible and biodegradable sensors, wide range (1 pM to 1 μM)	15 h	32
H_2O_2, glucose	Amperometry	Flexible sensors, good sensitivity (0.84, 5.6 μA/μM for H_2O_2 and glucose respectively), low LOD (50 μM for glucose)	30 days	232
Lactate, glucose, NO	Amperometry	Flexible sensors, good sensitivity (4.68, 3.21, 47 nA/μM for lactate, glucose, and NO respectively)	30 days	233
Glucose	Amperometry	Flexible and bioresorbable sensors, good sensitivity (0.2458 μA/mM), low LOD (0.1 mM), wide range (0−25 mM)	7 days	34
NO	Amperometry	Flexible and physically transient sensors, low LOD (3.92 nM), wide range (0.1−100 μM)	2 weeks	33
NO	OECT	Flexible sensors, good sensitivity (94 mV/dec), low LOD (3 nM), wide range (3 M to 100 μM)	8 days	234
Organic macromolecules				
HE4	Fluorescence	Good sensitivity (500 nM), low LOD (10 nM)	7 days	38
miRNA-21	Fluorescence	Biodegradable sensors, wide range (2.5−250 nM)	4 h	235
β-actin mRNA	Fluorescence	Biodegradable sensors, good reproducibility	35 days	236

fibroin to develop gallium arsenide microwave devices and transient resistive switching memory devices, respectively (Figure 4c (I and II)). Typical natural polymers degrade via enzymatic reactions, due to their stable backbone structure.[216] When enzymes are adsorbed on the surfaces of such polymers, they form enzyme−substrate complexes that function as biological catalysts capable of cleaving the polymer chains. Synthetically engineered polymers with fine-tunable physical and chemical characteristics, including poly lactic acid (PLA), poly glycolic acid (PGA), PVA, PCL, PGS, POC, PLGA, polyethylene glycol (PEG), polyethylene glycol diacrylate (PEGDA), among others, constitute a critical category of materials utilized in biodegradable implants.[217] They can be synthesized in a controlled manner with controlled degradation rate by various strategies. These include modulating chemical and physical properties such as composition, molecular weight, and crystallinity, as well as employing techniques like blending, copolymerization, and surface modification.[218] As shown in Figure 4c (III), the PVA substrate showed more rapid degradation in DI water at 15 °C by regulating its structural parameters using a 3D printer.[219] Biodegradable polymers such as PLGA[217] and chitosan/PVP substrates[220] have also been employed in flexible electronic devices and their swelling or degradation rates can be modulated by tuning the blending ratio (Figure 4c (IV and V)). Synthetic polymers with hydrolyzable labile ester, thioester, amide, anhydride bonds, etc., break down hydrolytically into oligomers or monomers that can be absorbed or excreted by the body.[221] This form of degradation in synthetic polymers occurs through surface and/or bulk erosion, depending on the matrix dimension and the relative rates of bond cleavage and water or enzyme diffusion inside the matrix.[222,223] Surface erosion, by transiently preserving the mechanical strength, molecular weight, and geometric shape of polymers, renders them suitable for use as protective encapsulation for implantable devices. For example, Kang et al.[186] has utilized a polyanhydride film to encapsulate implantable Si sensors for monitoring intracranial pressure and temperature. In contrast, bulk degradation gradually weakens the molecular weight and mechanical strength of polymers over time, resulting in structural failure and the accumulation of debris. Bioresorbable polymers such as PCL, PLGA, POC, silk fibroin, known for their bulk erosion characteristics, are widely adopted as substrates for implantable chemical sensors.[32,192,35,193] In addition to hydrolysis, oxidation can also represent a biologically relevant degradation mechanism. Activated inflammatory cells such as phagocytes, neutrophils, and foreign-body giant cells (FBGCs) release free radicals in the form of reactive oxygen or nitrogen species that can initiate the oxidation of polymers.[224]

4. REPRESENTATIVE IMPLANTABLE CHEMICAL SENSORS BASED ON FLEXIBLE AND/OR BIODEGRADABLE MATERIALS

Based on the aforementioned techniques, integrating flexible and/or biodegradable materials with chemical sensors can create significant opportunities for probing vital biomarkers in physiological environments. Target analytes of recently proposed implantable chemical sensors encompass ions (K^+, Na^+, Ca^{2+}, H^+), small molecules (DA, AA, H_2O_2, lactate, glucose, O_2, NO), and larger organic macromolecules (human epididymis protein (HE4), miRNA-21, β-actin messenger RNA (mRNA)),[225] are summarized in Table 3. These accomplished devices are critical to offer real-time monitoring for early diagnosis and disease treatment.[226,227]

4.1. Ions. Electrolytes play crucial roles in a myriad of physiological processes within the human body. Aberrations in ion concentrations within biofluids are frequently linked to increased morbidity and mortality rates within intensive care units.[237] The most prevalent ion-sensing devices are potentiometric instruments that have been modified using specific recognition chemistries (ionophores), or selective

https://doi.org/10.1021/acsnano.3c11832
ACS Nano 2024, 18, 3969−3995

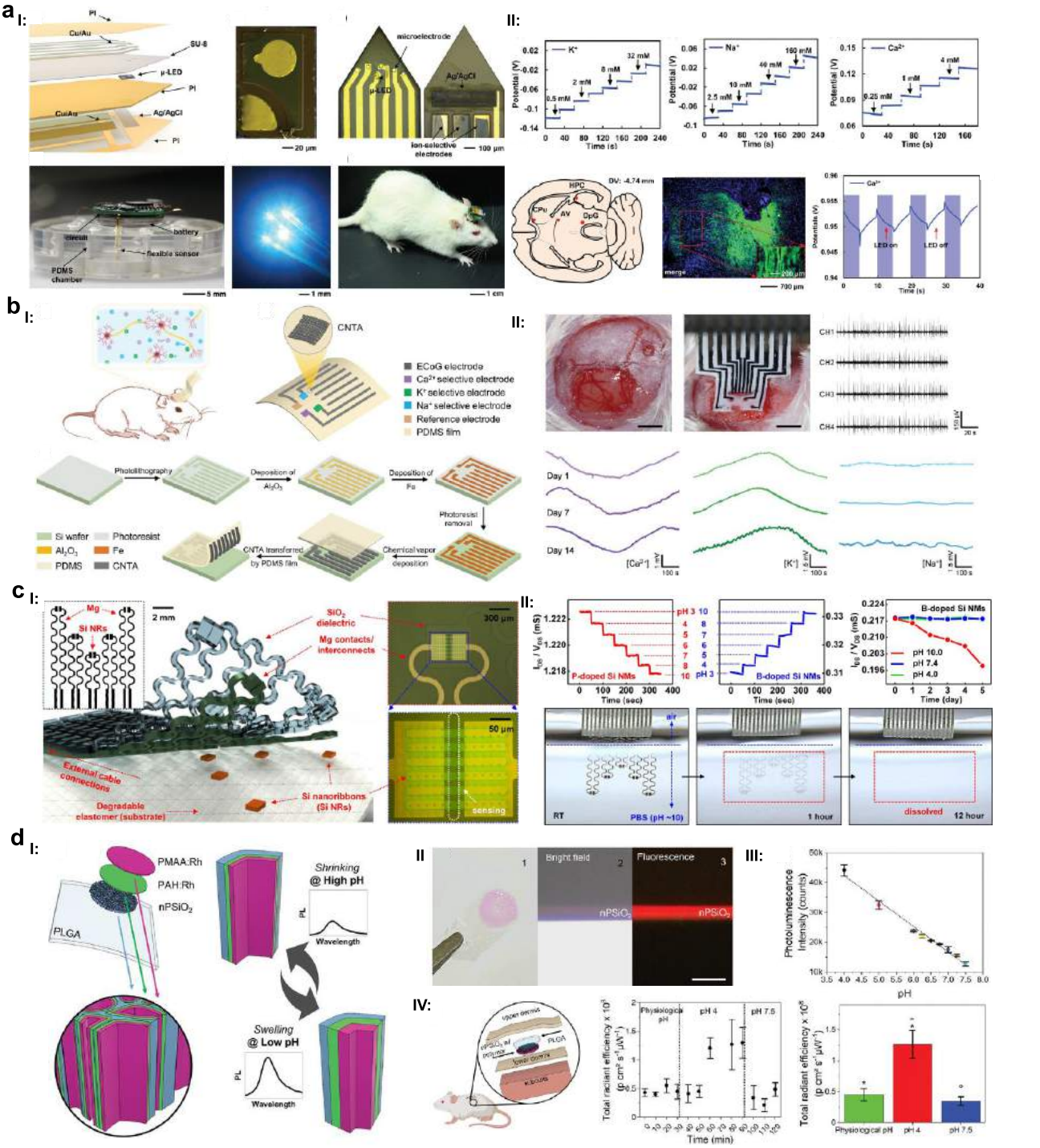

Figure 5. Representative implantable chemical sensors for ion detection. (a) A flexible electronic device with tentacle-like channels radiating from a central wireless circuit. (I) The configuration of the optoelectrical stimulation and biophysiological sensing device implanted within the rabbit brain; (II) The *in vitro* voltage response of ion sensing and *in vivo* measurement of Ca^{2+} upon optical stimulation. Reprinted with permission from ref [228]. Copyright 2020 Wiley-VCH. (b) Flexible multifunctional electrodes (FME) based on a carbon nanotube array (CNTA) to detect electrophysiology and ions. (I) Schematic diagram of the FME and the fabrication process of the CNTA electrode; (II) Electrophysiology recording and Ca^{2+}, K^+, Na^+ detection of the FME *in vivo*. Reprinted with permission from ref [229]. Copyright 2022 Wiley-VCH. (c) Schematic illustration of stretchable pH sensor built with doped silicon nanoribbons (Si NRs). (I) Exploded view and optical microscopic image of the pH sensor; (II) Measurement of conductance as a function of surrounding pH and the dissolution process of the sensor in PBS (pH 10). Reprinted with permission from ref [35]. Copyright 2015 American Chemical Society. (d) A bioresorbable nanostructured chemical sensor for monitoring of pH level *in vivo*. (I) Schematic diagram of the sensor structure and operation principle; (II) Bright-field and fluorescence optical microscope images of the nanostructured porous silicon oxide ($nPSiO_2$) scaffold coated with Rh-labeled polyelectrolytes; (III) Calibration curve of the bioresorbable pH sensor measured over the pH range of 4−7.5 in PBS at 37 °C; (IV) Schematic illustration of the sensor implanted in rodents and its steady-state fluorescence intensity, recorded across various pH environments. Reprinted with permission under a Creative Commons CC BY License from ref [37]. Copyright 2022 Wiley-VCH.

https://doi.org/10.1021/acsnano.3c11832
ACS Nano 2024, 18, 3969−3995

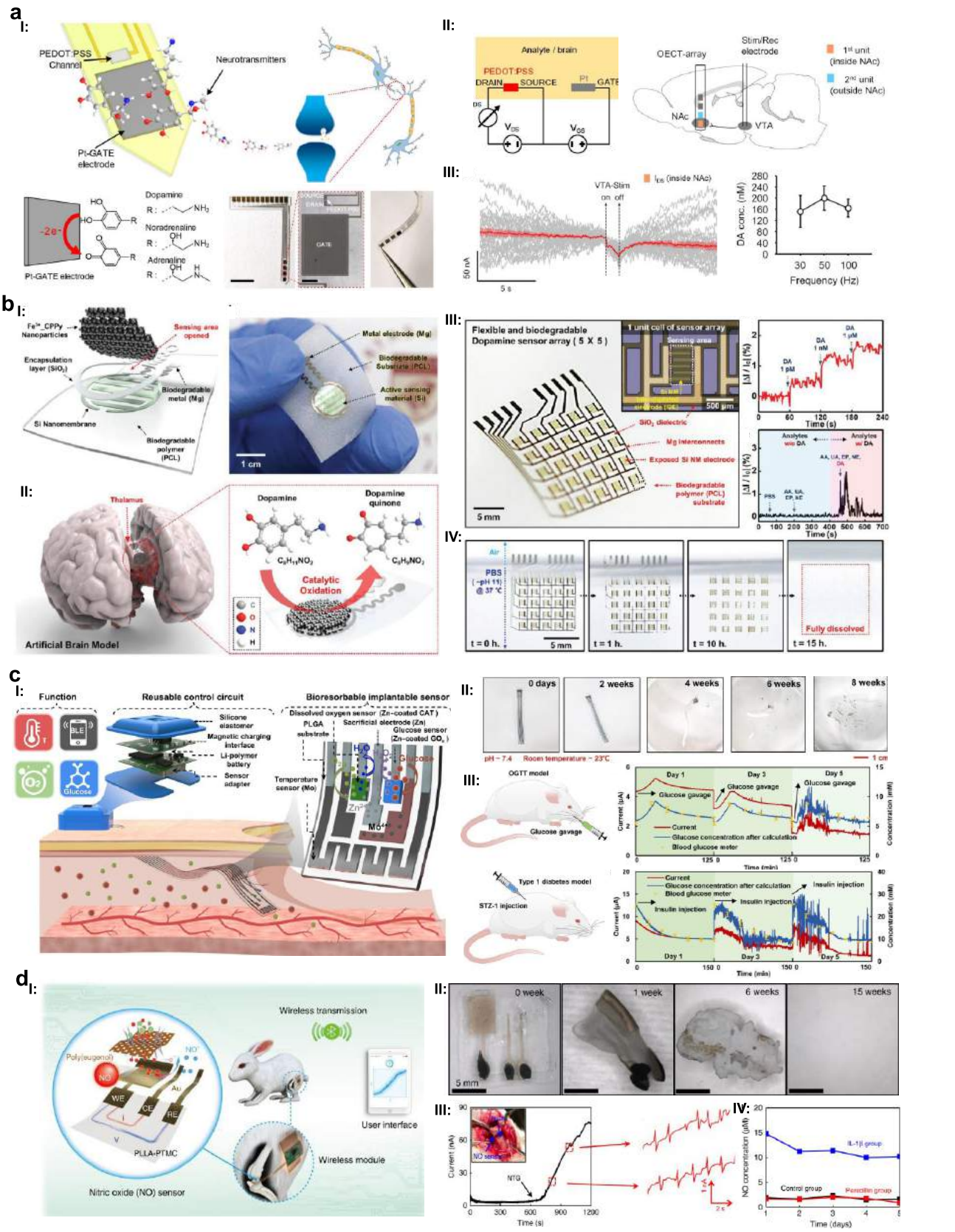

Figure 6. Representative implantable chemical sensors for small molecule detection. (a) Organic electrochemical transistor arrays (OECT-arrays) for real-time monitoring of catecholamine neurotransmitters (CA-NTs) *in vivo*. (I) Schematic diagram, photographs and working principle of OECT-array for CA-NT detection; (II) Schematic illustration and equivalent circuits showing the working setup of an OECT-array for mapping DA release around nucleus accumbens (NAc) region in response to neural stimulation of ventral tegmental area (VTA); (III) Current response (I_d) recorded by the OECT-array placed in NAc and associated DA concentrations in response to VTA stimulation at varying frequencies. Reprinted with permission under a Creative Commons CC BY 4.0 License [231]. Copyright 2020 eLife Sciences

https://doi.org/10.1021/acsnano.3c11832
ACS Nano 2024, 18, 3969−3995

Figure 6. continued

Publications. (b) Flexible DA sensor system. (I) Exploded view and a photograph depicting a DA sensor positioned on a flexible polycaprolactone (PCL) substrate; (II) Illustrations of the sensor implanted on the midbrain for detection of DA and associated chemical reactions at the surface of iron-decorated carboxylated polypyrrole (Fe^{3+}_C PPy) nanoparticles; (III) Photograph showcasing a 5 × 5 array of flexible, passively multiplexed electrodes, accompanied by the demonstration of amperometric and selective responses when immersed in PBS solutions; (IV) Sequential dissolution images of a DA sensor collected at different stages in PBS at body temperature (37 °C) under accelerated conditions (pH 11). Reprinted with permission from ref [32]. Copyright 2018 Wiley-VCH. (c) Bioresorbable electrochemical devices based on galvanic coupling for continuous glucose monitoring. (I) Schematic illustration and representative image of the electrochemical sensor; (II) The degradation of the bioresorbable glucose sensor in PBS solution; (III) *In vivo* evaluations of the bioresorbable electrochemical sensor. Reprinted with permission under a Creative Commons CC BY 4.0 License from ref [34]. Copyright 2023 American Association for the Advancement of Science. (d) A flexible and physically transient electrochemical sensor capable of nitric oxide (NO) monitoring. (I) Schematic illustration of a transient NO sensor composed of a bioresorbable PLLA−PTMC substrate, ultrathin Au nanomembrane electrodes, and a poly(eugenol) thin film; (II) Images collected at various stages of accelerated degradation of a NO sensor in PBS at 65 °C; (III) Real-time measurement of the current response of NO near the heart of the rabbit, stimulated by the intravenous infusion of nitroglycerine (NTG); (IV) Real-time monitoring of NO concentration over 5 days of implantation of the NO sensor in the joint cavity of a rabbit. Reprinted with permission under a Creative Commons CC BY License from ref [33]. Copyright 2023 Springer Nature.

membranes that selectively form complexes with target ions to generate a measurable electromotive force.[238] With recent advances in mesostructured materials and nanotechnologies, emerging optical biosensors have also been proposed to detect ions *in vivo*.[239]

For instance, Ling et al.[228] have developed flexible, tentacle-like channels using organic and inorganic materials in thin-film and nanoparticle formats for optoelectrical stimulation and ion monitoring. These flexible channels could be adaptively bent to accommodate different distances to the multiencephalic regions. As shown in Figure 5a (I), channels contained two stacked PI substrates that comprise a micro LED (μ-LED), four microelectrodes (30 μm in diameter) fabricated using Ti/Cu/Ti/Au multilayered architecture, and three ion-selective sensors. The potentiometric sensor exhibited linear response with increasing concentrations of K^+, Na^+, and Ca^{2+} and could record reversible alterations in Ca^{2+} concentration during recurring optical stimulation (Figure 5a (II)). Yang et al.[229] have engineered a flexible multifunctional electrode (FME) based on a carbon nanotube array (CNTA) to record electrocorticography (ECoG) and extracellular ions of Ca^{2+}, K^+, and Na^+. As depicted in Figure 5b (I), all electrodes were patterned onto a 170 μm-thick PDMS film to keep the FME self-standing for convenient implantation and accurate recording *in vivo*. The FME was carefully attached to the surface of the rat's cerebral cortex and achieved effective monitoring of ECoG and the detection of Ca^{2+}, K^+, and Na^+ for 2 weeks. (Figure 5b (II))

Sensing pH is an important application of implantable chemical sensors due to the highly regulated nature of H^+ concentration in blood plasma and several other body fluids, which can provide essential information on physiological environments.[9] Hwang et al.[35] have utilized a mesh design made of filamentary serpentine (FS) traces to create a flexible pH sensor capable of conformally laminating onto the time-dynamic, curvilinear surfaces of organs. As depicted in Figure 5c (I), doped Si NRs functionalized with 3-aminopropyltriethoxysilane (APTES) were used as flexible pH-sensitive probes.[35] Other components encompassed Mg electrodes and interconnections, SiO_2 interlayer dielectrics and encapsulation, as well as POC substrates. The $-NH_2$ and $-SiOH$ groups of APTES underwent protonation ($-NH_3^+$) at low pH and deprotonation ($-SiO^-$) at high pH. Measured changes in conductance (I_{ds}/V_{ds}) of the Si NRs defined the pH owing to charge accumulation or depletion (Figure 5c (II)). The pH sensor exhibited a marked decrease in the conductance in PBS (pH 10) owing to Mg erosion over 12 h and the gradual dissolution of POC, Si, and SiO_2 over several weeks. Fluorescence-based pH sensors have been predominantly proposed for localized measurements in tissues and organs, due to their high sensitivity and minimal demand for indicators. For instance, Corsi et al.[37] have developed a flexible, bioresorbable pH sensor, composed of a micrometer-thick membrane of nanostructured porous silica ($nPSiO_2$) coated with a nanometer-thick multilayer sensing component (Figure 5d (I and II)). The fluorescence intensity changed linearly in response to pH variations, due to swelling and shrinking of the polymer stack (Figure 5d (III)). The pH sensor was implanted in the subcutis on the back of mice and exhibited changes in fluorescence emission after the injection of different PBS solutions (pH 4 and 7.5) (Figure 5d (IV)).

4.2. Small Molecules. Small molecules such as metabolites (e.g., lactate, glucose, glutamate, DA) and biological gases (e.g., O_2, NO, CO_2) are critical to a number of physiological processes.[240] Various kinds of electrochemical sensors (including amperometric, voltammetric, potentiometric, and OECT-based sensors) are commonly employed to monitor these metabolites and gases.

Neurotransmitters like DA and 5-HT are crucial in the regulation of neural activity. Li et al.[230] have developed a graphene-based neural interface for monitoring monoamine neurotransmitters, including DA and 5-HT. This soft, flexible, and stretchable neurochemical sensor is constructed from graphene/iron oxide nanoparticle networks embedded within a polystyrene-*block*-poly(ethylene-*ran*-butylene)-*block*-polystyrene (SEBS) elastomer. Xie et al.[231] achieved OECT-arrays with Pt-GATE electrodes and a conductive PEDOT:PSS layer on a flexible polyethylene terephthalate (PET) substrate (Figure 6a (I)). The catecholamine neurotransmitters (CA-NT) oxidized to generate electrons on the surface of the Pt-GATE electrode to produce a measurable Faradaic current. Implanted into the rat brain's nucleus accumbens (NAc), the flexible OECT-array showed significant drain current reduction upon stimulation of the ventral tegmental area (VTA) (Figure 6a (II and III)). Kim et al.[32] have developed a flexible and biodegradable DA sensor, which was constructed by coating iron(III) carboxylated polypyrrole (Fe^{3+}_C PPy) nanoparticles onto Si NMs electrodes (Figure 6b (I)). Mg in serpentine 2D shapes served as electrical contacts and a flexible and biodegradable PCL film served as the substrate. The catalytic

https://doi.org/10.1021/acsnano.3c11832
ACS Nano 2024, 18, 3969−3995

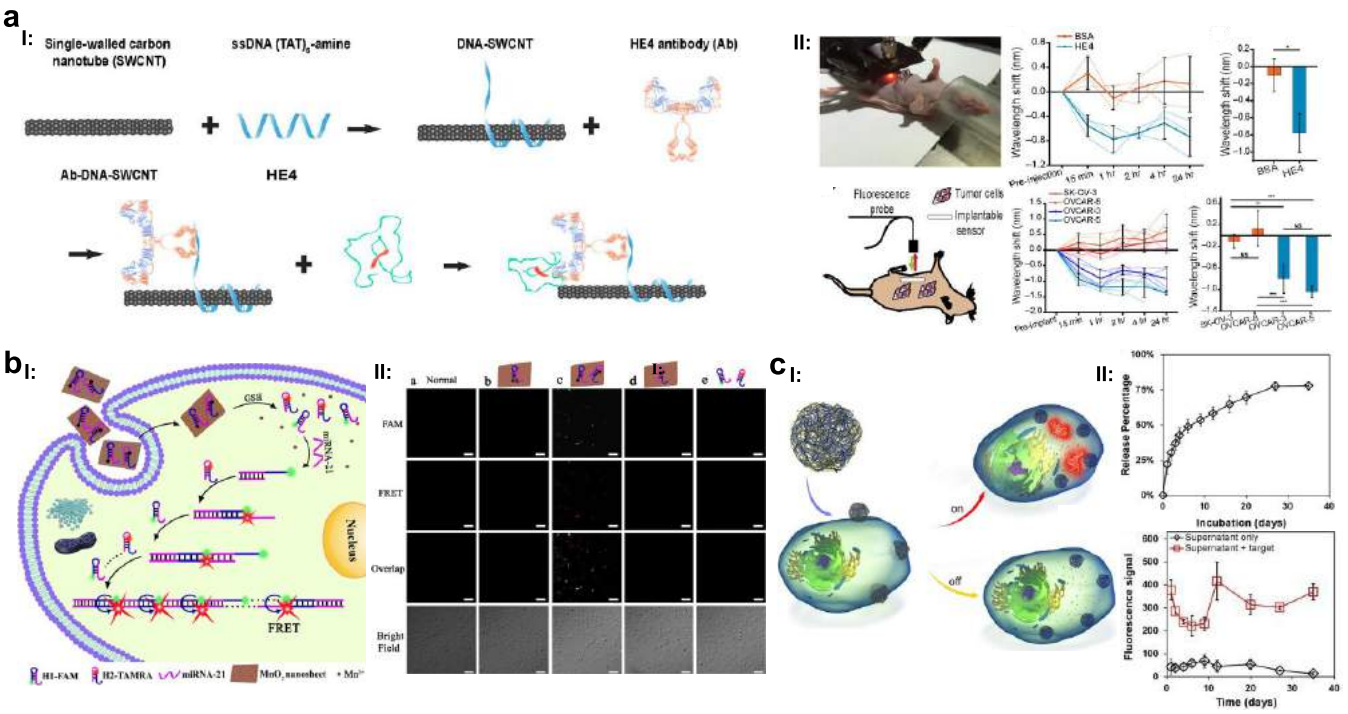

Figure 7. Representative implantable chemical sensors for organic macromolecules detection. (a) A prototype optical sensor for detecting ovarian cancer biomarker. (I) Schematic illustration of the synthesis and sensing mechanism of antibody-DNA-single-walled CNTs complex; (II) *In vivo* measurement of HE4 in orthotopic ovarian cancer models. Reprinted with permission under a Creative Commons CC BY 4.0 License from ref [38]. Copyright 2018 American Association for the Advancement of Science. (b) Biodegradable MnO_2 nanosheet-mediated sensors enable detection of intracellular microRNA. (I) Illustration of MnO_2 nanosheet-mediated in cell HCR signal enhancement for sensitively detecting miRNA-21 in living cells; (II) Confocal fluorescence images of miRNA-21 in HeLa cells incubated with different probes. Reprinted with permission from ref [235]. Copyright 2017 American Chemical Society. (c) A nanoparticle-based sensor platform for tracking (I) Schematic illustration of the nanosensor platform and intracellular implementation; (II) Sustained release of oligonucleotide molecular beacons (MBs) and their binding assay with β-actin mRNA. Reprinted with permission under a Creative Commons CC BY License from ref [236]. Copyright 2015 Springer Nature.

oxidation of DA triggered electron transfer to Si-NMs (Figure 6b (II)), altering their conductivity in respond to DA concentration. A 5 × 5 sensor array demonstrated high selectivity and sensitivity for DA detection, with constituent materials completely degraded after 15 h in PBS (pH 11) at 37 °C (Figure 6b (III and IV)).

The development of glucose sensors represents another critical domain of research, instrumental in the prevention, diagnosis, and treatment of diabetic ketoacidosis. Wang et al.[232] have developed functionalized helical fiber bundles of carbon nanotubes to continuously monitor multiple disease biomarkers such as Ca^{2+}, glucose, and H_2O_2. These compliant, lightweight, and flexible sensors mimicked muscle filaments and matched the bending stiffness of tissues and cells, ensuring a stable fiber-tissue interface. Li et al.[233] have developed an interface-stabilized fiber sensor (IEFS) for real-time monitoring of biochemical dynamics (e.g., glucose, lactate, NO, pH) in amniotic fluid during pregnancy to personalized prevention, diagnostic, and therapeutic of gestational diseases. IEFS was prepared by depositing sensing functional materials onto a flexible CNT fiber electrode. A restorative gel of collagen and silk fibroin was coated onto the twisted multiply fibers core, allowed for seamless integration with the amnion through gel adhesion. Efforts to eliminate the need to retrieve implanted devices have led to the development of bioresorbable glucose sensors. Li et al.[34] have developed a fully bioresorbable electrochemical sensor for CGM. As shown in Figure 6c (I), the sensor contained a glucose sensor, a dissolved oxygen (DO) sensor, and a temperature sensor fabricated on a PLGA substrate. The electrochemical sensor, connected with a flexible circuit board, could be deformed to fit implantation sites with minimal damage to dorsal subcutaneous tissues. After being immersed in PBS at RT, the constituent materials (e.g., Mo, W, Zn) gradually dissolved within 2 months (Figure 6c (II)). Real-time monitoring was conducted on rats and the biodegradable sensor successfully monitored the glucose level in 5 days following the administration of glucose and insulin (Figure 6c (III)).

Real-time tracking of NO levels in physiological environments is crucial for processes such as neurotransmission, immune responses, cardiovascular systems, angiogenesis, and joint circulation.[241] Li et al.[33] have utilized ultrathin patterned Au electrodes and a poly(L-lactic acid) and poly(trimethylene carbonate) (PLLA−PTMC) copolymer substrate to construct a biodegradable sensor for NO detection (Figure 6d (I)). As shown in Figure 6d (II), the device achieved full transience after 15 weeks in PBS solution at 65 °C. Real-time monitoring was performed on a rabbit's heart upon nitroglycerine (NTG) stimulation, a drug used for the treatment of angina pectoris, myocardial infarction, and chronic heart failure by releasing NO to dilate the vascular system.[242] Results indicated that the response current began to rise immediately upon NTG infusion (Figure 6d (III)). Additionally, the sensor implanted in a rabbit's joint cavity revealed significantly higher NO levels in the interleukin-1 beta (IL-1β) group (promoting inflammation after sensor implantation) compared to the control

https://doi.org/10.1021/acsnano.3c11832
ACS Nano 2024, 18, 3969−3995

(sensor implantation without treatment) and the penicillin (antibiotic treatment after sensor implantation) group. This indicated that inflammation in the joint cavity of the rabbit is associated with a high concentration of NO. Deng et al.[234] have reported an OECT device for real-time and wireless measurement of NO. This device was utilized to monitor the signals in the joint cavity of New Zealand white rabbits with anterior cruciate ligament (ACL) fracture for 8 days. The observed high levels of NO were associated with the onset of osteoarthritis (OA) at the later stage.

4.3. Organic Macromolecules. The precise detection of organic macromolecules holds significant potential for the early diagnosis of critical medical conditions, such as primary tumor formation. However, implantable electrochemical sensors designed for the detection of organic macromolecules, including proteins and nucleic acid, have been less explored compared to ions and small molecules. This is probably attributed to the challenges in achieving reliable affinity-based biorecognition elements (e.g., antibodies, aptamers) for macromolecules in biofluids, which face difficulties in overcoming biofoiling and enabling continuous monitoring with high sensitivity.[71,243] Therefore, the majority of electrochemical biosensing for biomacromolecules, such as proteins and nucleic acids, is currently limited to in vitro laboratory assay settings or wearable electronics. For example, Liu et al.[244] have proposed an OECT-based sensor to perform fast in vitro detection of SARS-CoV-2 immunoglobulin G (IgG) for COVID-19. SARS-CoV-2 spike protein served as the recognition element and can successfully detect SARS-CoV-2 IgG through antigen−antibody reactions with an ultralow detection limit of 1 fM. Tu et al.[245] have proposed a wearable patch that can achieve wireless and continuous monitoring of C-reactive protein (CRP) in sweat based on graphene sensor array and anti-CRP capture antibodies. The detection of CRP in the sweat has been confirmed and was related to chronic and acute diseases associated with inflammation.

By contrast, optical sensing methods are less susceptible to nonspecific binding and real-time detection of organic macromolecules in physiological environments can be implemented. For example, the advancement of sensors targeting HE4 has garnered significant interest, and proven to be important in detecting early stage disease to reduce the burden of ovarian cancer. Williams et al.[38] have engineered a prototype fluorescence-based optical sensor composed of an antibody-functionalized CNTs complex, which responds quantitatively to HE4 via modulation of the nanotube optical bandgap. As depicted in Figure 7a (I), the DNA-single wall carbon nanotube (SWCNT) complexes were conjugated to a goat polyclonal anti-HE4 IgG antibody. The antibody-nanotube complex responded to HE4 via modulation of the nanotube emission wavelength. Fluorescence was captured from live mice using a fiber optic probe-based system, as presented in Figure 7a (II). The implanted sensors displayed a prominent blue-shift within 15 min with the injection of HE4 and HE4-expressing ovarian cancer cells (OVCAR-3 and OVCAR-5).

MicroRNAs (miRNAs) are key regulators in processes like cell differentiation, proliferation, and apoptosis, modulating gene expression by either promoting target mRNA degradation or inhibiting its translation.[246] Li et al.[235] have introduced a fluorescence resonance energy transfer (FRET)-based biosensor to track miRNA-21 in living cells based on biodegradable manganese dioxide (MnO_2) nanosheet-mediated and target-triggered assembly of hairpins. Intracellular glutathione (GSH) degrades the MnO_2 nanosheets to release the two free hairpin DNA probes (H1-FAM and H2-TMR), resulting in significantly amplified FRET signals for detecting trace miRNA-21 in cells (Figure 7b (I)). When HeLa cells were exposed to H1-FAM/H2-TMR/MnO_2 nanosheets, distinct red emissions were evident (Figure 7b (II)). This arises as the targeted miRNA-21 instigates the assembly of the liberated H1-FAM and H2-TMR into double-stranded (dsDNA) polymers. Subsequently, this positions FAM and TMR in close proximity, facilitating efficient FRET, which resulted in the emission of red fluorescence. Yeo et al.[236] have reported the detection of β-actin mRNA by encapsulating oligonucleotide molecular beacon (MBs)-based nanosensors within biodegradable PLGA nanoparticles (Figure 7c (I)). Sustained release of ∼75% of encapsulated MBs from nanosensors was observed over 35 days. Upon hybridization with β-actin mRNA, MBs matched the β-actin mRNA sequence, resulting in about an 8-fold increase in fluorescence signal (Figure 7c (II)).

5. CHALLENGES AND PERSPECTIVES

In this review, we discuss pioneering research on the approaches to building implantable chemical sensors based on flexible and biodegradable materials, highlighting their potential in diagnostic and therapeutic applications. The adjustable mechanical properties, favorable biocompatibility, and degradation characteristics eliminating materials retention and secondary surgeries for device retraction enable innovative sensing platforms for continuous monitoring of vital biomarkers in complex biological environments. Despite notable advancements, there are crucial challenges that remain to be addressed to further advance implantable chemical sensors.

The capabilities of implantable flexible and biodegradable chemical sensors are currently limited in terms of the types of analytes that can be monitored. To expand their applications, it is crucial to explore a wider range of biomarkers, including metabolites, hormones, and proteins. This necessitates the development of reliable affinity-based biorecognition elements that can counteract nonspecific binding, including proteins, aptamers, and artificial receptors (e.g., molecularly imprinted polymers (MIPs)).[247] The enhancement of both the reversibility and stability of bioaffinity receptors is critical. In particular, the ability to rapidly reset the interactions between the bioreceptors and target molecules by adjusting the intermolecular forces, using methods such as the application of heat, electric fields, or chemicals, is essential.[1,243] Ongoing advancements in bioreceptors that offer rapid regeneration and antifouling properties will support continuous detection of target analytes.

Advancements are needed in the field of versatile flexible conductive and semiconductive materials with mechanical properties better suited for specific implantation sites. Through molecular engineering, the characteristics of polymeric materials such as conjugated polymers and supramolecular polymers can be tailored to meet desired properties like flexibility, stretchability, conductivity, and adhesiveness.[248,249] Alternative material options include intrinsically soft materials such as hydrogels, which mimic biological tissues, and liquid metals that allow for free deformation.[250,251] However, the properties of these materials still lag behind those of traditional inorganic electronic materials, and there is a need to develop

https://doi.org/10.1021/acsnano.3c11832
ACS Nano 2024, 18, 3969−3995

manufacturing techniques that can meet the standards of existing technology. Conversely, adapting conventional electronic materials to formats that are relevant to biological systems can capitalize on their high performance and compatibility with established manufacturing processes.[122] Additionally, the material requirements for various implant sites differ. For instance, sensors implanted in the brain necessitate an ultralow modulus to be compatible with the brain's soft tissue,[252] stretchability becomes a crucial factor in highly mobile body regions (e.g., spinal cord, legs), whereas stability in highly corrosive conditions is essential for materials used in the gastrointestinal tract.[253] Ultimately, by integrating these soft and hard materials for different application scenarios, it is possible to create sensor-biology interfaces that offer both biomimetic integration and high-fidelity performance.

Enhancing stability of flexible and bioresorbable chemical sensors remains a challenge. Developing materials strategies that provide desirable antibiofouling properties and stable recognition elements is crucial. A 3D porous conductive matrix incorporated with antifouling agents (e.g., bovine serum albumin) has been shown to effectively reduce nonspecific binding while preserving electron conduction.[71] The integration of nanoporous membranes that enhance enzyme immobilization efficacy, as well as the use of artificial receptors like MIPs, could contribute to long-term sensor stability.[254,255] For biodegradable chemical sensors, achieving controllable material degradation that aligns with the operational lifespan of the device and ensuring complete degradation afterward presents another challenge. Employing active components that degrade more slowly and have a greater thickness, along with the appropriate use of encapsulating polymeric materials, can effectively prolong the operational timeline of a device. Additionally, integrating stimuli-responsive materials may further enhance stability and facilitate smart, on-demand degradation of the device.[256] Strategies aimed at device miniaturization, minimizing foreign body responses, and improving interface adhesion are also important considerations. These approaches would facilitate seamless integration with biological tissues and enhance the long-term stability and sensitivity of implantable chemical sensors.

Most current implantable chemical sensors rely on percutaneous connections for power supply and data recording. However, future development of wireless circuits and power devices in a flexible and/or bioresorbable format can enable long-term biomarker detection in a nontethered manner and improve patient compliance. Wireless circuits provide advantages such as freedom from spatial constraints, improved device efficiency, extended lifespan of the host, and a lowered risk of infection.[257] Although the power supply for most conventional wireless devices relies on batteries,[258] battery-free approaches offer advantages like lightweight design, small form factor, and the ability for full implantation.[259] Inductive coupling and radio frequency (RF) transmission represent the most widely utilized battery-free wireless techniques for power supply and data communication.[260] However, the rigid structures of most wireless circuits impose significant mechanical mismatch, potentially causing tissue damage.[261] The integration of serpentine metal thin-film traces on soft substrates with off-the-shelf electronics components can potentially address these issues.[262] For instance, a wireless, fully implantable, and stretchable optogenetic stimulator based on RF power harvesting has been demonstrated.[263] In addition, other power supply techniques could also provide alternative solutions, including ultrasound,[264] magnetoelectrics,[265] etc. Furthermore, the development of biodegradable power sources such as inductive coils,[266] batteries,[267] and supercapacitors[268] is essential to enable next-generation biodegradable and fully implantable sensor systems.

Integrating implantable chemical sensors with flexible and biodegradable therapeutic systems, such as electrical stimulation or programmable drug delivery systems, can create closed-loop systems that enable timely intervention based on the detection of abnormal biomarkers. For instance, the electrical stimulation of injured nerve tissues has shown effectiveness in improving and accelerating the recovery.[266] Closed-loop drug delivery systems combining an implantable sensor and a drug delivery apparatus enable timely pharmacotherapy.[269] A commercial example of this is the MiniMed 670G system,[270] which automatically adjusts insulin doses based on continuous blood glucose level measurements from an implantable sensor. Moreover, coupling these sensors with innovative data mining and machine learning techniques can realize intelligent analysis of recorded information, leading to the identification of disease patterns for early intervention.

Overall, accomplishing these goals requires collaborative efforts among materials science, electrical engineering, biomedical engineering, and related disciplines. The ultimate result would be highly integrated and multiplexed implantable chemical sensor platforms with flexible and bioresorbable features that can seamlessly adapt to biological systems. These platforms would provide crucial information for advanced early diagnosis and treatment of diseases.

AUTHOR INFORMATION

Corresponding Author

Lan Yin − *School of Materials Science and Engineering, The Key Laboratory of Advanced Materials of Ministry of Education, State Key Laboratory of New Ceramics and Fine Processing, Laboratory of Flexible Electronics Technology, Tsinghua University, Beijing 100084, P. R. China;* orcid.org/0000-0001-7306-4628; Email: lanyin@tsinghua.edu.cn

Authors

Chen Hu − *School of Materials Science and Engineering, The Key Laboratory of Advanced Materials of Ministry of Education, State Key Laboratory of New Ceramics and Fine Processing, Laboratory of Flexible Electronics Technology, Tsinghua University, Beijing 100084, P. R. China*

Liu Wang − *Key Laboratory of Biomechanics and Mechanobiology of Ministry of Education, Beijing Advanced Innovation Center for Biomedical Engineering, School of Biological Science and Medical Engineering, Beihang University, Beijing 100083, P. R. China*

Shangbin Liu − *School of Materials Science and Engineering, The Key Laboratory of Advanced Materials of Ministry of Education, State Key Laboratory of New Ceramics and Fine Processing, Laboratory of Flexible Electronics Technology, Tsinghua University, Beijing 100084, P. R. China*

Xing Sheng − *Department of Electronic Engineering, Beijing National Research Center for Information Science and Technology, Institute for Precision Medicine, Laboratory of Flexible Electronics Technology, IDG/McGovern Institute for Brain Research, Tsinghua University, Beijing 100084, P. R. China;* orcid.org/0000-0002-8744-1700

Complete contact information is available at:

https://doi.org/10.1021/acsnano.3c11832
ACS Nano 2024, 18, 3969−3995

https://pubs.acs.org/10.1021/acsnano.3c11832

Author Contributions

‖Chen Hu, Liu Wang, and Shangbin Liu contributed equally to this work.

Notes

The authors declare no competing financial interest.

ACKNOWLEDGMENTS

The project was supported by the National Natural Science Foundation of China (T2122010 and 52171239 to L.Y., 32101088 to L.W., 52272277 to X.S.), Beijing Municipal Natural Science Foundation (Z220015 to L.Y.), Beijing Nova Program and Fundamental Research Funds for the Central Universities.

VOCABULARY

Limit of detection (LoD): The minimum concentration of an analyte capable of generating a consistently detectable signal.

Selectivity: The sensor's capacity to differentiate between the analyte and possibly unknown potential interferences.

Stability: The ability of a sensor to maintain precise measurements in both short-term and long-term durations within an uncontrolled environment.

Flexibility: The quality or capability of being easily adaptable, pliable, or malleable readily to varied conditions circumstances or requirements.

Biodegradability: A property of the material that can undergo decomposition into biomass and gases under biologically benign or physiological conditions.

REFERENCES

(1) Sempionatto, J. R.; Lasalde-Ramírez, J. A.; Mahato, K.; Wang, J.; Gao, W. Wearable Chemical Sensors for Biomarker Discovery in the Omics Era. *Nat. Rev. Chem.* **2022**, *6*, 899−915.

(2) Abdul-Aziz, M. H.; Alffenaar, J.-W. C.; Bassetti, M.; Bracht, H.; Dimopoulos, G.; Marriott, D.; Neely, M. N.; Paiva, J.-A.; Pea, F.; Sjovall, F.; et al. Antimicrobial Therapeutic Drug Monitoring in Critically Ill Adult Patients: A Position Paper. *Intensive Care Med.* **2020**, *46*, 1127−1153.

(3) Soto, R. J.; Hall, J. R.; Brown, M. D.; Taylor, J. B.; Schoenfisch, M. H. In Vivo Chemical Sensors: Role of Biocompatibility on Performance and Utility. *Anal. Chem.* **2017**, *89*, 276−299.

(4) Hong, Y. J.; Jeong, H.; Cho, K. W.; Lu, N.; Kim, D. H. Wearable and Implantable Devices for Cardiovascular Healthcare: From Monitoring to Therapy Based on Flexible and Stretchable Electronics. *Adv. Funct. Mater.* **2019**, *29*, 1808247.

(5) Ming Li, C.; Dong, H.; Cao, X.; Luong, J. H. T.; Zhang, X. Implantable Electrochemical Sensors for Biomedical and Clinical Applications: Progress, Problems, and Future Possibilities. *Curr. Med. Chem.* **2007**, *14*, 937−951.

(6) Archana, V.; Xia, Y.; Fang, R.; Gnana Kumar, G. Hierarchical Cuo/Nio-Carbon Nanocomposite Derived from Metal Organic Framework on Cello Tape for the Flexible and High Performance Nonenzymatic Electrochemical Glucose Sensors. *ACS Sustainable Chem. Eng.* **2019**, *7*, 6707−6719.

(7) Zhang, Y.; Li, N.; Xiang, Y.; Wang, D.; Zhang, P.; Wang, Y.; Lu, S.; Xu, R.; Zhao, J. A Flexible Non-Enzymatic Glucose Sensor Based on Copper Nanoparticles Anchored on Laser-Induced Graphene. *Carbon* **2020**, *156*, 506−513.

(8) Liang, T.; Zou, L.; Guo, X.; Ma, X.; Zhang, C.; Zou, Z.; Zhang, Y.; Hu, F.; Lu, Z.; Tang, K.; Li, C. M. Rising Mesopores to Realize Direct Electrochemistry of Glucose Oxidase toward Highly Sensitive Detection of Glucose. *Adv. Funct. Mater.* **2019**, *29*, 1903026.

(9) Kellum, J. A. Determinants of Blood Ph in Health and Disease. *Crit. Care* **2000**, *4*, 6.

(10) Bi, X.; Hartono, D.; Yang, K. L. Real-Time Liquid Crystal Ph Sensor for Monitoring Enzymatic Activities of Penicillinase. *Adv. Funct. Mater.* **2009**, *19*, 3760−3765.

(11) Hao, G.; Xu, Z. P.; Li, L. Manipulating Extracellular Tumour Ph: An Effective Target for Cancer Therapy. *RSC Adv.* **2018**, *8*, 22182−22192.

(12) Qin, M.; Guo, H.; Dai, Z.; Yan, X.; Ning, X. Advances in Flexible and Wearable Ph Sensors for Wound Healing Monitoring. *J. Semicond.* **2019**, *40*, 111607.

(13) Flinck, M.; Kramer, S.; Pedersen, S. Roles of Ph in Control of Cell Proliferation. *Acta Physiol.* **2018**, *223*, No. e13068.

(14) Cuartero, M.; Parrilla, M.; Crespo, G. A. Wearable Potentiometric Sensors for Medical Applications. *Sensors* **2019**, *19*, 363.

(15) Diringer, M. Neurologic Manifestations of Major Electrolyte Abnormalities. *Handbook of clinical neurology* **2017**, *141*, 705−713.

(16) Jin, P.; Munson, J. M. Fluids and Flows in Brain Cancer and Neurological Disorders. *WIREs Mech. Dis.* **2023**, *15*, No. e1582.

(17) Joseph, J. I. Review of the Long-Term Implantable Senseonics Continuous Glucose Monitoring System and Other Continuous Glucose Monitoring Systems. *J. Diabetes Sci. Technol.* **2021**, *15*, 167−173.

(18) Marty, P.; Roquilly, A.; Vallée, F.; Luzi, A.; Ferré, F.; Fourcade, O.; Asehnoune, K.; Minville, V. Lactate Clearance for Death Prediction in Severe Sepsis or Septic Shock Patients During the First 24 h in Intensive Care Unit: An Observational Study. *Ann. Intensive Care* **2013**, *3*, 1−7.

(19) Rabinowitz, J. D.; Enerbäck, S. Lactate: The Ugly Duckling of Energy Metabolism. *Nat. Metab.* **2020**, *2*, 566−571.

(20) Zhang, J.; Xu, J.; Lim, J.; Nolan, J. K.; Lee, H.; Lee, C. H. Wearable Glucose Monitoring and Implantable Drug Delivery Systems for Diabetes Management. *Adv. Healthcare Mater.* **2021**, *10*, 2100194.

(21) Beardslee, L. A.; Banis, G. E.; Chu, S.; Liu, S.; Chapin, A. A.; Stine, J. M.; Pasricha, P. J.; Ghodssi, R. Ingestible Sensors and Sensing Systems for Minimally Invasive Diagnosis and Monitoring: The Next Frontier in Minimally Invasive Screening. *ACS Sens.* **2020**, *5*, 891−910.

(22) Lee, H.; Lee, Y.; Song, C.; Cho, H. R.; Ghaffari, R.; Choi, T. K.; Kim, K. H.; Lee, Y. B.; Ling, D.; Lee, H.; et al. An Endoscope with Integrated Transparent Bioelectronics and Theranostic Nanoparticles for Colon Cancer Treatment. *Nat. Commun.* **2015**, *6*, 10059.

(23) Yoo, S.; Lee, J.; Joo, H.; Sunwoo, S. H.; Kim, S.; Kim, D. H. Wireless Power Transfer and Telemetry for Implantable Bioelectronics. *Adv. Healthcare Mater.* **2021**, *10*, 2100614.

(24) Cha, K. H.; Wang, X.; Meyerhoff, M. E. Nitric Oxide Release for Improving Performance of Implantable Chemical Sensors-a Review. *Appl. Mater. Today* **2017**, *9*, 589−597.

(25) Li, C.; Guo, C.; Fitzpatrick, V.; Ibrahim, A.; Zwierstra, M. J.; Hanna, P.; Lechtig, A.; Nazarian, A.; Lin, S. J.; Kaplan, D. L. Design of Biodegradable, Implantable Devices Towards Clinical Translation. *Nat. Rev. Mater.* **2020**, *5*, 61−81.

(26) Han, W. B.; Lee, J. H.; Shin, J. W.; Hwang, S. W. Advanced Materials and Systems for Biodegradable, Transient Electronics. *Adv. Mater.* **2020**, *32*, 2002211.

(27) Min, J.; Jung, Y.; Ahn, J.; Lee, J. G.; Lee, J.; Ko, S. H. Recent Advances in Biodegradable Green Electronic Materials and Sensor Applications. *Adv. Mater.* **2023**, *35*, 2211273.

(28) Won, D.; Bang, J.; Choi, S. H.; Pyun, K. R.; Jeong, S.; Lee, Y.; Ko, S. H. Transparent Electronics for Wearable Electronics Application. *Chem. Rev.* **2023**, *123*, 9982−10078.

(29) Lin, T.; Xu, Y.; Zhao, A.; He, W.; Xiao, F. Flexible Electrochemical Sensors Integrated with Nanomaterials for in Situ Determination of Small Molecules in Biological Samples: A Review. *Anal. Chim. Acta* **2022**, *1207*, 339461.

(30) Nasiri, S.; Khosravani, M. R. Progress and Challenges in Fabrication of Wearable Sensors for Health Monitoring. *Sens. Actuators, A* **2020**, *312*, 112105.
(31) Chang, J. K.; Chang, H. P.; Guo, Q.; Koo, J.; Wu, C. I.; Rogers, J. A. Biodegradable Electronic Systems in 3d, Heterogeneously Integrated Formats. *Adv. Mater.* **2018**, *30*, 1704955.
(32) Kim, H. S.; Yang, S. M.; Jang, T. M.; Oh, N.; Kim, H. S.; Hwang, S. W. Bioresorbable Silicon Nanomembranes and Iron Catalyst Nanoparticles for Flexible, Transient Electrochemical Dopamine Monitors. *Adv. Healthcare Mater.* **2018**, *7*, 1801071.
(33) Li, R.; Qi, H.; Ma, Y.; Deng, Y.; Liu, S.; Jie, Y.; Jing, J.; He, J.; Zhang, X.; Wheatley, L.; et al. A Flexible and Physically Transient Electrochemical Sensor for Real-Time Wireless Nitric Oxide Monitoring. *Nat. Commun.* **2020**, *11*, 3207.
(34) Li, J.; Liu, J.; Wu, Z.; Shang, X.; Li, Y.; Huo, W.; Huang, X. Fully Printed and Self-Compensated Bioresorbable Electrochemical Devices Based on Galvanic Coupling for Continuous Glucose Monitoring. *Sci. Adv.* **2023**, *9*, No. eadi3839.
(35) Hwang, S.-W.; Lee, C. H.; Cheng, H.; Jeong, J.-W.; Kang, S.-K.; Kim, J.-H.; Shin, J.; Yang, J.; Liu, Z.; Ameer, G. A.; et al. Biodegradable Elastomers and Silicon Nanomembranes/Nanoribbons for Stretchable, Transient Electronics, and Biosensors. *Nano Lett.* **2015**, *15*, 2801−2808.
(36) Dou, Q.; Hu, D.; Gao, H.; Zhang, Y.; Yetisen, A. K.; Butt, H.; Wang, J.; Nie, G.; Dai, Q. High Performance Boronic Acid-Containing Hydrogel for Biocompatible Continuous Glucose Monitoring. *RSC Adv.* **2017**, *7*, 41384−41390.
(37) Corsi, M.; Paghi, A.; Mariani, S.; Golinelli, G.; Debrassi, A.; Egri, G.; Leo, G.; Vandini, E.; Vilella, A.; Dähne, L.; et al. Bioresorbable Nanostructured Chemical Sensor for Monitoring of Ph Level in Vivo. *Adv. Sci.* **2022**, *9*, 2202062.
(38) Williams, R. M.; Lee, C.; Galassi, T. V.; Harvey, J. D.; Leicher, R.; Sirenko, M.; Dorso, M. A.; Shah, J.; Olvera, N.; Dao, F.; et al. Noninvasive Ovarian Cancer Biomarker Detection Via an Optical Nanosensor Implant. *Sci. Adv.* **2018**, *4*, No. eaaq1090.
(39) Inda-Webb, M.; Jimenez, M.; Liu, Q.; Phan, N.; Ahn, J.; Steiger, C.; Wentworth, A.; Riaz, A.; Zirtiloglu, T.; Wong, K.; et al. Sub-1.4 Cm3 Capsule for Detecting Labile Inflammatory Biomarkers in Situ. *Nature* **2023**, *620*, 386.
(40) Tao, L.; Kong, Y.; Xiang, Y.; Cao, Y.; Ye, X.; Liu, Z. Implantable Optical Fiber Microelectrode with Anti-Biofouling Ability for in Vivo Photoelectrochemical Analysis. *Chin. Chem. Lett.* **2023**, *34*, 107481.
(41) Wu, J.; Liu, H.; Chen, W.; Ma, B.; Ju, H. Device Integration of Electrochemical Biosensors. *Nat. Rev. Bioeng.* **2023**, *1*, 346−360.
(42) Herbert, R.; Lim, H. R.; Park, S.; Kim, J. H.; Yeo, W. H. Recent Advances in Printing Technologies of Nanomaterials for Implantable Wireless Systems in Health Monitoring and Diagnosis. *Adv. Healthcare Mater.* **2021**, *10*, 2100158.
(43) Li, J.; Cheng, Y.; Gu, M.; Yang, Z.; Zhan, L.; Du, Z. Sensing and Stimulation Applications of Carbon Nanomaterials in Implantable Brain-Computer Interface. *Int. J. Mol. Sci.* **2023**, *24*, 5182.
(44) Ding, J.; Qin, W. Recent Advances in Potentiometric Biosensors. *TrAC, Trends Anal. Chem.* **2020**, *124*, 115803.
(45) Wei, H.; Li, L.; Jin, J.; Wu, F.; Yu, P.; Ma, F.; Mao, L. Galvanic Redox Potentiometry Based Microelectrode Array for Synchronous Ascorbate and Single-Unit Recordings in Rat Brain. *Anal. Chem.* **2020**, *92*, 10177−10182.
(46) Bobacka, J. Conducting Polymer-Based Solid-State Ion-Selective Electrodes. *Electroanalysis* **2006**, *18*, 7−18.
(47) Wang, L.; Chen, J.; Wang, J.; Li, H.; Chen, C.; Feng, J.; Guo, Y.; Yu, H.; Sun, X.; Peng, H. Flexible Dopamine-Sensing Fiber Based on Potentiometric Method for Long-Term Detection in Vivo. *Sci. China Chem.* **2021**, *64*, 1763−1769.
(48) Tahirbegi, I. B.; Alvira, M.; Mir, M.; Samitier, J. Simple and Fast Method for Fabrication of Endoscopic Implantable Sensor Arrays. *Sensors* **2014**, *14*, 11416−11426.
(49) Singh, P.; Pandey, S. K.; Singh, J.; Srivastava, S.; Sachan, S.; Singh, S. K. Biomedical Perspective of Electrochemical Nano-biosensor. *Nano-Micro Lett.* **2016**, *8*, 193−203.
(50) Vashist, S. K. Continuous Glucose Monitoring Systems: A Review. *Diagnostics* **2013**, *3*, 385−412.
(51) Baig, N.; Sajid, M.; Saleh, T. A. Recent Trends in Nanomaterial-Modified Electrodes for Electroanalytical Applications. *TrAC, Trends Anal. Chem.* **2019**, *111*, 47−61.
(52) Pu, Z.; Tu, J.; Han, R.; Zhang, X.; Wu, J.; Fang, C.; Wu, H.; Zhang, X.; Yu, H.; Li, D. A Flexible Enzyme-Electrode Sensor with Cylindrical Working Electrode Modified with a 3d Nanostructure for Implantable Continuous Glucose Monitoring. *Lab Chip* **2018**, *18*, 3570−3577.
(53) Zhu, J.; Liu, S.; Hu, Z.; Zhang, X.; Yi, N.; Tang, K.; Dexheimer, M. G.; Lian, X.; Wang, Q.; Yang, J.; et al. Laser-Induced Graphene Non-Enzymatic Glucose Sensors for on-Body Measurements. *Biosens. Bioelectron.* **2021**, *193*, 113606.
(54) Choi, H.; Shin, H.; Cho, H. U.; Blaha, C. D.; Heien, M. L.; Oh, Y.; Lee, K. H.; Jang, D. P. Neurochemical Concentration Prediction Using Deep Learning Vs Principal Component Regression in Fast Scan Cyclic Voltammetry: A Comparison Study. *ACS Chem. Neurosci.* **2022**, *13*, 2288−2297.
(55) Nur Topkaya, S.; Cetin, A. E. Electrochemical Aptasensors for Biological and Chemical Analyte Detection. *Electroanalysis* **2021**, *33*, 277−291.
(56) Martins, F. C.; Pimenta, L. C.; De Souza, D. Antidepressants Determination Using an Electroanalytical Approach: A Review of Methods. *J. Pharm. Biomed. Anal.* **2021**, *206*, 114365.
(57) Gao, W.; Nyein, H. Y.; Shahpar, Z.; Fahad, H. M.; Chen, K.; Emaminejad, S.; Gao, Y.; Tai, L.-C.; Ota, H.; Wu, E.; et al. Wearable Microsensor Array for Multiplexed Heavy Metal Monitoring of Body Fluids. *ACS Sens.* **2016**, *1*, 866−874.
(58) Ariño, C.; Banks, C. E.; Bobrowski, A.; Crapnell, R. D.; Economou, A.; Królicka, A.; Pérez-Ràfols, C.; Soulis, D.; Wang, J. Electrochemical Stripping Analysis. *Nat. Rev. Methods Primers* **2022**, *2*, 62.
(59) Janegitz, B. C.; Silva, T. A.; Wong, A.; Ribovski, L.; Vicentini, F. C.; Sotomayor, M. d. P. T.; Fatibello-Filho, O. The Application of Graphene for in Vitro and in Vivo Electrochemical Biosensing. *Biosens. Bioelectron.* **2017**, *89*, 224−233.
(60) Liao, W.; Cui, X. T. Reagentless Aptamer Based Impedance Biosensor for Monitoring a Neuro-Inflammatory Cytokine Pdgf. *Biosens. Bioelectron.* **2007**, *23*, 218−224.
(61) Zou, Y.; Wang, J.; Guan, S.; Zou, L.; Gao, L.; Li, H.; Fang, Y.; Wang, C. Anti-Fouling Peptide Functionalization of Ultraflexible Neural Probes for Long-Term Neural Activity Recordings in the Brain. *Biosens. Bioelectron.* **2021**, *192*, 113477.
(62) Ghosh, E.; Egunov, A. I.; Karnaushenko, D.; Medina-Sánchez, M.; Schmidt, O. G. Self-Assembled Sensor-in-a-Tube as a Versatile Tool for Label-Free Eis Viability Investigation of Cervical Cancer Cells. *Frequenz* **2022**, *76*, 729−740.
(63) Hedayatipour, A.; Aslanzadeh, S.; McFarlane, N. Cmos Based Whole Cell Impedance Sensing: Challenges and Future Outlook. *Biosens. Bioelectron.* **2019**, *143*, 111600.
(64) Yun, J.; Hong, Y.-T.; Hong, K.-H.; Lee, J.-H. Ex Vivo Identification of Thyroid Cancer Tissue Using Electrical Impedance Spectroscopy on a Needle. *Sens. Actuators, B* **2018**, *261*, 537−544.
(65) Park, J.; Choi, W.-M.; Kim, K.; Jeong, W.-I.; Seo, J.-B.; Park, I. Biopsy Needle Integrated with Electrical Impedance Sensing Micro-electrode Array Towards Real-Time Needle Guidance and Tissue Discrimination. *Sci. Rep.* **2018**, *8*, 264.
(66) Lim, J. M.; Kim, J. H.; Ryu, M. Y.; Cho, C. H.; Park, T. J.; Park, J. P. An Electrochemical Peptide Sensor for Detection of Dengue Fever Biomarker Ns1. *Anal. Chim. Acta* **2018**, *1026*, 109−116.
(67) Wan, Y.; Zhang, D.; Wang, Y.; Hou, B. A 3d-Impedimetric Immunosensor Based on Foam Ni for Detection of Sulfate-Reducing Bacteria. *Electrochem. Commun.* **2010**, *12*, 288−291.
(68) Nguyen, K. T.; Kim, H. Y.; Park, J.-O.; Choi, E.; Kim, C.-S. Tripolar Electrode Electrochemical Impedance Spectroscopy for Endoscopic Devices toward Early Colorectal Tumor Detection. *ACS Sens.* **2022**, *7*, 632−640.

https://doi.org/10.1021/acsnano.3c11832
ACS Nano 2024, 18, 3969−3995

(69) Stupin, D. D.; Kuzina, E. A.; Abelit, A. A.; Emelyanov, A. K.; Nikolaev, D. M.; Ryazantsev, M. N.; Koniakhin, S. V.; Dubina, M. V. Bioimpedance Spectroscopy: Basics and Applications. *ACS Biomater. Sci. Eng.* **2021**, *7*, 1962−1986.
(70) Gao, F.; Song, J.; Zhang, B.; Tanaka, H.; Gao, F.; Qiu, W.; Wang, Q. Synthesis of Core-Shell Structured Au@ Bi2s3 Nanorod and Its Application as DNA Immobilization Matrix for Electrochemical Biosensor Construction. *Chin. Chem. Lett.* **2020**, *31*, 181−184.
(71) Sabatédel Río, J.; Henry, O. Y.; Jolly, P.; Ingber, D. E. An Antifouling Coating That Enables Affinity-Based Electrochemical Biosensing in Complex Biological Fluids. *Nat. Nanotechnol.* **2019**, *14*, 1143−1149.
(72) Jung, S. H.; Han, H. S.; Kim, Y. B.; Kim, D. S.; Deshpande, N. G.; Oh, S. J.; Choi, J. H.; Cho, H. K. Toward Ultraviolet Solution Processed Zrox/Izo Transistors with Top-Gate and Dual-Gate Operation: Selection of Solvents, Precursors, Stabilizers, and Additive Elements. *J. Alloys Compd.* **2020**, *847*, 156431.
(73) Poghossian, A.; Schöning, M. J. Label-Free Sensing of Biomolecules with Field-Effect Devices for Clinical Applications. *Electroanalysis* **2014**, *26*, 1197−1213.
(74) Wong, W. S.; Raychaudhuri, S.; Lujan, R.; Sambandan, S.; Street, R. A. Hybrid Si Nanowire/Amorphous Silicon Fets for Large-Area Image Sensor Arrays. *Nano Lett.* **2011**, *11*, 2214−2218.
(75) Fahad, H. M.; Hussain, M. M. High-Performance Silicon Nanotube Tunneling Fet for Ultralow-Power Logic Applications. *IEEE Trans. Electron Devices* **2013**, *60*, 1034−1039.
(76) Liu, J.; Chen, X.; Wang, Q.; Xiao, M.; Zhong, D.; Sun, W.; Zhang, G.; Zhang, Z. Ultrasensitive Monolayer Mos2 Field-Effect Transistor Based DNA Sensors for Screening of Down Syndrome. *Nano Lett.* **2019**, *19*, 1437−1444.
(77) Xu, S.; Zhan, J.; Man, B.; Jiang, S.; Yue, W.; Gao, S.; Guo, C.; Liu, H.; Li, Z.; Wang, J.; Zhou, Y. Real-Time Reliable Determination of Binding Kinetics of DNA Hybridization Using a Multi-Channel Graphene Biosensor. *Nat. Commun.* **2017**, *8*, 14902.
(78) Zhou, S.; Xiao, M.; Liu, F.; He, J.; Lin, Y.; Zhang, Z. Sub-10 Parts Per Billion Detection of Hydrogen with Floating Gate Transistors Built on Semiconducting Carbon Nanotube Film. *Carbon* **2021**, *180*, 41−47.
(79) Dai, X.; Vo, R.; Hsu, H.-H.; Deng, P.; Zhang, Y.; Jiang, X. Modularized Field-Effect Transistor Biosensors. *Nano Lett.* **2019**, *19*, 6658−6664.
(80) Zhou, Y.; Liu, B.; Lei, Y.; Tang, L.; Li, T.; Yu, S.; Zhang, G. J.; Li, Y. T. Acupuncture Needle-Based Transistor Neuroprobe for in Vivo Monitoring of Neurotransmitter. *Small* **2022**, *18*, 2204142.
(81) Tian, B.; Cohen-Karni, T.; Qing, Q.; Duan, X.; Xie, P.; Lieber, C. M. Three-Dimensional, Flexible Nanoscale Field-Effect Transistors as Localized Bioprobes. *Science* **2010**, *329*, 830−834.
(82) Reiner-Rozman, C.; Larisika, M.; Nowak, C.; Knoll, W. Graphene-Based Liquid-Gated Field Effect Transistor for Biosensing: Theory and Experiments. *Biosens. Bioelectron.* **2015**, *70*, 21−27.
(83) Torricelli, F.; Adrahtas, D. Z.; Bao, Z.; Berggren, M.; Biscarini, F.; Bonfiglio, A.; Bortolotti, C. A.; Frisbie, C. D.; Macchia, E.; Malliaras, G. G.; et al. Electrolyte-Gated Transistors for Enhanced Performance Bioelectronics. *Nat. Rev. Methods Primers* **2021**, *1*, 66.
(84) Chen, H.; Choo, T. K.; Huang, J.; Wang, Y.; Liu, Y.; Platt, M.; Palaniappan, A.; Liedberg, B.; Tok, A. I. Y. Label-Free Electronic Detection of Interleukin-6 Using Horizontally Aligned Carbon Nanotubes. *Mater. Des.* **2016**, *90*, 852−857.
(85) Gualandi, I.; Tessarolo, M.; Mariani, F.; Tonelli, D.; Fraboni, B.; Scavetta, E. Organic Electrochemical Transistors as Versatile Analytical Potentiometric Sensors. *Front. Bioeng. Biotechnol.* **2019**, *7*, 354.
(86) Li, J.; Madiyar, F.; Ghate, S.; Kumar, K. S.; Thomas, J. Plasmonic Organic Electrochemical Transistors for Enhanced Sensing. *Nano Res.* **2023**, *16*, 3201−3206.
(87) Chen, S.; Surendran, A.; Wu, X.; Leong, W. L. Contact Modulated Ionic Transfer Doping in All-Solid-State Organic Electrochemical Transistor for Ultra-High Sensitive Tactile Perception at Low Operating Voltage. *Adv. Funct. Mater.* **2020**, *30*, 2006186.
(88) Fauzi, F.; Rianjanu, A.; Santoso, I.; Triyana, K. Gas and Humidity Sensing with Quartz Crystal Microbalance (Qcm) Coated with Graphene-Based Materials-a Mini Review. *Sens. Actuators, A* **2021**, *330*, 112837.
(89) Srivastava, A.; Sakthivel, P. Quartz-Crystal Microbalance Study for Characterizing Atomic Oxygen in Plasma Ash Tools. *J. Vac. Sci. Technol., A* **2001**, *19*, 97−100.
(90) Liao, Z.; Zhang, Y.; Li, Y.; Miao, Y.; Gao, S.; Lin, F.; Deng, Y.; Geng, L. Microfluidic Chip Coupled with Optical Biosensors for Simultaneous Detection of Multiple Analytes: A Review. *Biosens. Bioelectron.* **2019**, *126*, 697−706.
(91) Vavrinsky, E.; Esfahani, N. E.; Hausner, M.; Kuzma, A.; Rezo, V.; Donoval, M.; Kosnacova, H. The Current State of Optical Sensors in Medical Wearables. *Biosensors* **2022**, *12*, 217.
(92) Shi, Y.; Hu, Y.; Jiang, N.; Yetisen, A. K. Fluorescence Sensing Technologies for Ophthalmic Diagnosis. *ACS Sens.* **2022**, *7*, 1615−1633.
(93) Rzhechitskiy, Y.; Gurkov, A.; Bolbat, N.; Shchapova, E.; Nazarova, A.; Timofeyev, M.; Borvinskaya, E. Adipose Fin as a Natural "Optical Window" for Implantation of Fluorescent Sensors into Salmonid Fish. *Animals* **2022**, *12*, 3042.
(94) Calabretta, M. M.; Zangheri, M.; Calabria, D.; Lopreside, A.; Montali, L.; Marchegiani, E.; Trozzi, I.; Guardigli, M.; Mirasoli, M.; Michelini, E. Based Immunosensors with Bio-Chemiluminescence Detection. *Sensors* **2021**, *21*, 4309.
(95) Shu, J.; Tang, D. Recent Advances in Photoelectrochemical Sensing: From Engineered Photoactive Materials to Sensing Devices and Detection Modes. *Anal. Chem.* **2020**, *92*, 363−377.
(96) Qiu, Z.; Tang, D. Nanostructure-Based Photoelectrochemical Sensing Platforms for Biomedical Applications. *J. Mater. Chem. B* **2020**, *8*, 2541−2561.
(97) Zhou, Q.; Tang, D. Recent Advances in Photoelectrochemical Biosensors for Analysis of Mycotoxins in Food. *TrAC, Trends Anal. Chem.* **2020**, *124*, 115814.
(98) Ma, X.; Kang, J.; Wu, Y.; Pang, C.; Li, S.; Li, J.; Xiong, Y.; Luo, J.; Wang, M.; Xu, Z. Recent Advances in Metal/Covalent Organic Framework-Based Materials for Photoelectrochemical Sensing Applications. *TrAC, Trends Anal. Chem.* **2022**, *157*, 116793.
(99) Li, C.; Cai, Y.; Pang, M.; Zhou, X.; Luo, X.; Xiao, Z. A Coumarin-Appended Cyclometalated Iridium (Iii) Complex for Visible Light Driven Photoelectrochemical Bioanalysis. *Biosens. Bioelectron.* **2020**, *147*, 111779.
(100) Hu, X.; Wang, Y.; Zuping, X.; Song, P.; Wang, A.-J.; Qian, Z.; Yuan, P.-X.; Zhao, T.; Feng, J.-J. Novel Aggregation-Enhanced Pec Photosensitizer Based on Electrostatic Linkage of Ionic Liquid with Protoporphyrin Ix for Ultrasensitive Detection of Molt-4 Cells. *Anal. Chem.* **2022**, *94*, 3708−3717.
(101) Li, Y.; Wang, W.; Gong, H.; Xu, J.; Yu, Z.; Wei, Q.; Tang, D. Graphene-Coated Copper-Doped Zno Quantum Dots for Sensitive Photoelectrochemical Bioanalysis of Thrombin Triggered by DNA Nanoflowers. *J. Mater. Chem. B* **2021**, *9*, 6818−6824.
(102) Polat, E. O.; Mercier, G.; Nikitskiy, I.; Puma, E.; Galan, T.; Gupta, S.; Montagut, M.; Piqueras, J. J.; Bouwens, M.; Durduran, T.; et al. Flexible Graphene Photodetectors for Wearable Fitness Monitoring. *Sci. Adv.* **2019**, *5*, No. eaaw7846.
(103) Çakıroğlu, B.; Demirci, Y. C.; Gökgöz, E.; Özacar, M. A Photoelectrochemical Glucose and Lactose Biosensor Consisting of Gold Nanoparticles, Mno2 and G-C3n4 Decorated Tio2. *Sens. Actuators, B* **2019**, *282*, 282−289.
(104) Ge, L.; Xu, Y.; Ding, L.; You, F.; Liu, Q.; Wang, K. Perovskite-Type Bifeo3/Ultrathin Graphite-Like Carbon Nitride Nanosheets Pn Heterojunction: Boosted Visible-Light-Driven Photoelectrochemical Activity for Fabricating Ampicillin Aptasensor. *Biosens. Bioelectron.* **2019**, *124*, 33−39.
(105) Li, M.; Tian, X.; Liang, W.; Yuan, R.; Chai, Y. Ultrasensitive Photoelectrochemical Assay with Ptb7-Th/Cdte Quantum Dots Sensitized Structure as Signal Tag and Benzo-4-Chlorohexadienone

Precipitate as Efficient Quencher. *Anal. Chem.* **2018**, *90*, 14521−14526.
(106) Zhu, L.-B.; Lu, L.; Wang, H.-Y.; Fan, G.-C.; Chen, Y.; Zhang, J.-D.; Zhao, W.-W. Enhanced Organic- Inorganic Heterojunction of Polypyrrole@ Bi2wo6: Fabrication and Application for Sensitive Photoelectrochemical Immunoassay of Creatine Kinase-Mb. *Biosens. Bioelectron.* **2019**, *140*, 111349.
(107) Li, X.; Lu, Y.; Liu, Q. Electrochemical and Optical Biosensors Based on Multifunctional Mxene Nanoplatforms: Progress and Prospects. *Talanta* **2021**, *235*, 122726.
(108) Eivazzadeh-Keihan, R.; Saadatidizaji, Z.; Maleki, A.; de la Guardia, M. d. l.; Mahdavi, M.; Barzegar, S.; Ahadian, S. Recent Progresses in Development of Biosensors for Thrombin Detection. *Biosensors* **2022**, *12*, 767.
(109) Svitkova, V.; Palchetti, I. Functional Polymers in Photoelectrochemical Biosensing. *Bioelectrochemistry* **2020**, *136*, 107590.
(110) Hu, F. X.; Miao, J.; Guo, C.; Yang, H. B.; Liu, B. Real-Time Photoelectrochemical Quantification of Hydrogen Peroxide Produced by Living Cells. *Chem. Eng. J.* **2021**, *407*, 127203.
(111) Devadoss, A.; Sudhagar, P.; Terashima, C.; Nakata, K.; Fujishima, A. Photoelectrochemical Biosensors: New Insights into Promising Photoelectrodes and Signal Amplification Strategies. *J. Photochem. Photobiol., C* **2015**, *24*, 43−63.
(112) Li, L.; Zhang, Y.; Yan, Z.; Chen, M.; Zhang, L.; Zhao, P.; Yu, J. Ultrasensitive Photoelectrochemical Detection of Microrna on Paper by Combining a Cascade Nanozyme-Engineered Biocatalytic Precipitation Reaction and Target-Triggerable DNA Motor. *ACS Sens.* **2020**, *5*, 1482−1490.
(113) Liu, K.; Deng, H.; Wang, Y.; Cheng, S.; Xiong, X.; Li, C. A Sandwich-Type Photoelectrochemical Immunosensor Based on Res2 Nanosheets for High-Performance Determination of Carcinoembryonic Antigen. *Sens. Actuators, B* **2020**, *320*, 128341.
(114) Tang, Y.; Liu, Y.; Wang, J.; Wang, J.; Liu, Z. In Vivo Tracking of Persistent Organic Pollutants Via a Coaxially Integrated and Implanted Photofuel Microsensor. *Environ. Sci. Technol.* **2023**, *57*, 2826−2836.
(115) Guan, X.; Deng, X.; Song, J.; Wang, X.; Wu, S. Polydopamine with Tailorable Photoelectrochemical Activities for the Highly Sensitive Immunoassay of Tumor Markers. *Anal. Chem.* **2021**, *93*, 6763−6769.
(116) Li, J.; Lin, X.; Zhang, Z.; Tu, W.; Dai, Z. Red Light-Driven Photoelectrochemical Biosensing for Ultrasensitive and Scatheless Assay of Tumor Cells Based on Hypotoxic Agins2 Nanoparticles. *Biosens. Bioelectron.* **2019**, *126*, 332−338.
(117) Chen, Y.; Zhou, S.; Li, L.; Zhu, J.-j. Nanomaterials-Based Sensitive Electrochemiluminescence Biosensing. *Nano Today* **2017**, *12*, 98−115.
(118) Li, L.; Chen, Y.; Zhu, J.-J. Recent Advances in Electrochemiluminescence Analysis. *Anal. Chem.* **2017**, *89*, 358−371.
(119) Liu, Z.; Qi, W.; Xu, G. Recent Advances in Electrochemiluminescence. *Chem. Soc. Rev.* **2015**, *44*, 3117−3142.
(120) Han, C.; Guo, W. Fluorescent Noble Metal Nanoclusters Loaded Protein Hydrogel Exhibiting Anti-Biofouling and Self-Healing Properties for Electrochemiluminescence Biosensing Applications. *Small* **2020**, *16*, 2002621.
(121) Cao, Y.; Wang, J. X.; Lin, C.; Geng, Y. Q.; Ma, C.; Zhu, J. J.; Wang, L.; Zhu, W. Zwitterionic Electrochemiluminescence Biointerface Contributes to Label-Free Monitoring of Exosomes Dynamics in a Fluidic Microreaction Device. *Adv. Funct. Mater.* **2023**, *33*, 2214294.
(122) Luo, Y.; Abidian, M. R.; Ahn, J.-H.; Akinwande, D.; Andrews, A. M.; Antonietti, M.; Bao, Z.; Berggren, M.; Berkey, C. A.; Bettinger, C. J.; et al. Technology Roadmap for Flexible Sensors. *ACS Nano* **2023**, *17*, 5211−5295.
(123) Song, E.; Li, J.; Won, S. M.; Bai, W.; Rogers, J. A. Materials for Flexible Bioelectronic Systems as Chronic Neural Interfaces. *Nat. Mater.* **2020**, *19*, 590−603.
(124) Choi, Y. S.; Yin, R. T.; Pfenniger, A.; Koo, J.; Avila, R.; Benjamin Lee, K.; Chen, S. W.; Lee, G.; Li, G.; Qiao, Y.; et al. Fully Implantable and Bioresorbable Cardiac Pacemakers without Leads or Batteries. *Nat. Biotechnol.* **2021**, *39*, 1228−1238.
(125) Li, H.; Ma, Y.; Huang, Y. Material Innovation and Mechanics Design for Substrates and Encapsulation of Flexible Electronics: A Review. *Mater. Horiz.* **2021**, *8*, 383−400.
(126) Yao, S.; Ren, P.; Song, R.; Liu, Y.; Huang, Q.; Dong, J.; O'Connor, B. T.; Zhu, Y. Nanomaterial-Enabled Flexible and Stretchable Sensing Systems: Processing, Integration, and Applications. *Adv. Mater.* **2020**, *32*, 1902343.
(127) McAlpine, M. C.; Ahmad, H.; Wang, D.; Heath, J. R. Highly Ordered Nanowire Arrays on Plastic Substrates for Ultrasensitive Flexible Chemical Sensors. *Nat. Mater.* **2007**, *6*, 379−384.
(128) VanDersarl, J. J.; Mercanzini, A.; Renaud, P. Integration of 2d and 3d Thin Film Glassy Carbon Electrode Arrays for Electrochemical Dopamine Sensing in Flexible Neuroelectronic Implants. *Adv. Funct. Mater.* **2015**, *25*, 78−84.
(129) Qian, G.; Liao, X.; Zhu, Y.; Pan, F.; Chen, X.; Yang, Y. Designing Flexible Lithium-Ion Batteries by Structural Engineering. *ACS Energy Lett.* **2019**, *4*, 690−701.
(130) Liu, Y.; He, K.; Chen, G.; Leow, W. R.; Chen, X. Nature-Inspired Structural Materials for Flexible Electronic Devices. *Chem. Rev.* **2017**, *117*, 12893−12941.
(131) Rogers, J. A.; Someya, T.; Huang, Y. Materials and Mechanics for Stretchable Electronics. *Science* **2010**, *327*, 1603−1607.
(132) Song, J.; Feng, X.; Huang, Y. Mechanics and Thermal Management of Stretchable Inorganic Electronics. *Natl. Sci. Rev.* **2016**, *3*, 128−143.
(133) Bowden, N.; Brittain, S.; Evans, A. G.; Hutchinson, J. W.; Whitesides, G. M. Spontaneous Formation of Ordered Structures in Thin Films of Metals Supported on an Elastomeric Polymer. *Nature* **1998**, *393*, 146−149.
(134) Sun, Y.; Choi, W. M.; Jiang, H.; Huang, Y. Y.; Rogers, J. A. Controlled Buckling of Semiconductor Nanoribbons for Stretchable Electronics. *Nat. Nanotechnol.* **2006**, *1*, 201−207.
(135) Jiang, H.; Sun, Y.; Rogers, J. A.; Huang, Y. Mechanics of Precisely Controlled Thin Film Buckling on Elastomeric Substrate. *Appl. Phys. Lett.* **2007**, DOI: 10.1063/1.2719027.
(136) Jung, W.-B.; Cho, S.-Y.; Yun, G.-T.; Choi, J.; Kim, Y.; Kim, M.; Kang, H.; Jung, H.-T. Hierarchical Metal Oxide Wrinkles as Responsive Chemical Sensors. *ACS Appl. Nano Mater.* **2019**, *2*, 5520−5526.
(137) Rogers, J.; Huang, Y.; Schmidt, O. G.; Gracias, D. H. Origami Mems and Nems. *MRS Bull.* **2016**, *41*, 123−129.
(138) Xu, S.; Yan, Z.; Jang, K.-I.; Huang, W.; Fu, H.; Kim, J.; Wei, Z.; Flavin, M.; McCracken, J.; Wang, R.; et al. Assembly of Micro/Nanomaterials into Complex, Three-Dimensional Architectures by Compressive Buckling. *Science* **2015**, *347*, 154−159.
(139) Zhang, M.; Sun, J. J.; Khatib, M.; Lin, Z.-Y.; Chen, Z.-H.; Saliba, W.; Gharra, A. l.; Horev, Y. D.; Kloper, V.; Milyutin, Y.; et al. Time-Space-Resolved Origami Hierarchical Electronics for Ultrasensitive Detection of Physical and Chemical Stimuli. *Nat. Commun.* **2019**, *10*, 1120.
(140) Zhang, Y.; Yan, Z.; Nan, K.; Xiao, D.; Liu, Y.; Luan, H.; Fu, H.; Wang, X.; Yang, Q.; Wang, J.; et al. A Mechanically Driven Form of Kirigami as a Route to 3d Mesostructures in Micro/Nanomembranes. *Proc. Natl. Acad. Sci. U. S. A.* **2015**, *112*, 11757−11764.
(141) Gao, B.; Elbaz, A.; He, Z.; Xie, Z.; Xu, H.; Liu, S.; Su, E.; Liu, H.; Gu, Z. Bioinspired Kirigami Fish-Based Highly Stretched Wearable Biosensor for Human Biochemical-Physiological Hybrid Monitoring. *Adv. Mater. Technol.* **2018**, *3*, 1700308.
(142) Won, P.; Park, J. J.; Lee, T.; Ha, I.; Han, S.; Choi, M.; Lee, J.; Hong, S.; Cho, K.-J.; Ko, S. H. Stretchable and Transparent Kirigami Conductor of Nanowire Percolation Network for Electronic Skin Applications. *Nano Lett.* **2019**, *19*, 6087−6096.
(143) Xu, Y.; Zhang, B. Recent Advances in Porous Pt-Based Nanostructures: Synthesis and Electrochemical Applications. *Chem. Soc. Rev.* **2014**, *43*, 2439−2450.
(144) Zhang, S.; Jiang, W.; Li, Y.; Yang, X.; Sun, P.; Liu, F.; Yan, X.; Gao, Y.; Liang, X.; Ma, J.; Lu, G. Highly-Sensitivity Acetone Sensors

Based on Spinel-Type Oxide (Nife2o4) through Optimization of Porous Structure. *Sens. Actuators, B* **2019**, *291*, 266−274.
(145) Harraz, F. A. Porous Silicon Chemical Sensors and Biosensors: A Review. *Sens. Actuators, B* **2014**, *202*, 897−912.
(146) Casanova, A.; Iniesta, J.; Gomis-Berenguer, A. Recent Progress in the Development of Porous Carbon-Based Electrodes for Sensing Applications. *Analyst* **2022**, *147*, 767−783.
(147) Davoodi, E.; Montazerian, H.; Haghniaz, R.; Rashidi, A.; Ahadian, S.; Sheikhi, A.; Chen, J.; Khademhosseini, A.; Milani, A. S.; Hoorfar, M.; Toyserkani, E. 3d-Printed Ultra-Robust Surface-Doped Porous Silicone Sensors for Wearable Biomonitoring. *ACS Nano* **2020**, *14*, 1520−1532.
(148) Zhou, H. C.; Long, J. R.; Yaghi, O. M. Introduction to Metal-Organic Frameworks. *Chem. Rev.* **2012**, *112*, 673−674.
(149) Li, Y.; Ling, W.; Liu, X.; Shang, X.; Zhou, P.; Chen, Z.; Xu, H.; Huang, X. Metal-Organic Frameworks as Functional Materials for Implantable Flexible Biochemical Sensors. *Nano Res.* **2021**, *14*, 2981−3009.
(150) Ling, W.; Hao, Y.; Wang, H.; Xu, H.; Huang, X. A Novel Cu-Metal-Organic Framework with Two-Dimensional Layered Topology for Electrochemical Detection Using Flexible Sensors. *Nanotechnology* **2019**, *30*, 424002.
(151) Ling, W.; Liew, G.; Li, Y.; Hao, Y.; Pan, H.; Wang, H.; Ning, B.; Xu, H.; Huang, X. Materials and Techniques for Implantable Nutrient Sensing Using Flexible Sensors Integrated with Metal-Organic Frameworks. *Adv. Mater.* **2018**, *30*, 1800917.
(152) Lee, J.; Noh, J.-S.; Lee, S. H.; Song, B.; Jung, H.; Kim, W.; Lee, W. Cracked Palladium Films on an Elastomeric Substrate for Use as Hydrogen Sensors. *Int. J. Hydrogen Energy* **2012**, *37*, 7934−7939.
(153) Jaiswal, M.; Menon, R. Polymer Electronic Materials: A Review of Charge Transport. *Polym. Int.* **2006**, *55*, 1371−1384.
(154) Sarkar, B.; Satapathy, D. K.; Jaiswal, M. Nanostructuring Mechanical Cracks in a Flexible Conducting Polymer Thin Film for Ultra-Sensitive Vapor Sensing. *Nanoscale* **2019**, *11*, 200−210.
(155) Gray, D. S.; Tien, J.; Chen, C. S. High-Conductivity Elastomeric Electronics. *Adv. Mater.* **2004**, *16*, 393−397.
(156) Tseng, P.; Napier, B.; Garbarini, L.; Kaplan, D. L.; Omenetto, F. G. Functional, Rf-Trilayer Sensors for Tooth-Mounted, Wireless Monitoring of the Oral Cavity and Food Consumption. *Adv. Mater.* **2018**, *30*, 1703257.
(157) Li, D.; Yu, S.; Sun, C.; Zou, C.; Yu, H.; Xu, K. U-Shaped Fiber-Optic Atr Sensor Enhanced by Silver Nanoparticles for Continuous Glucose Monitoring. *Biosens. Bioelectron.* **2015**, *72*, 370−375.
(158) Mishra, R. K.; Hubble, L. J.; Martín, A.; Kumar, R.; Barfidokht, A.; Kim, J.; Musameh, M. M.; Kyratzis, I. L.; Wang, J. Wearable Flexible and Stretchable Glove Biosensor for on-Site Detection of Organophosphorus Chemical Threats. *ACS Sens.* **2017**, *2*, 553−561.
(159) Yang, Y.; Song, Y.; Bo, X.; Min, J.; Pak, O. S.; Zhu, L.; Wang, M.; Tu, J.; Kogan, A.; Zhang, H.; et al. A Laser-Engraved Wearable Sensor for Sensitive Detection of Uric Acid and Tyrosine in Sweat. *Nat. Biotechnol.* **2020**, *38*, 217−224.
(160) Pham, T. A.; Nguyen, T. K.; Vadivelu, R. K.; Dinh, T.; Qamar, A.; Yadav, S.; Yamauchi, Y.; Rogers, J. A.; Nguyen, N. T.; Phan, H. P. A Versatile Sacrificial Layer for Transfer Printing of Wide Bandgap Materials for Implantable and Stretchable Bioelectronics. *Adv. Funct. Mater.* **2020**, *30*, 2004655.
(161) Bai, W.; Yang, H.; Ma, Y.; Chen, H.; Shin, J.; Liu, Y.; Yang, Q.; Kandela, I.; Liu, Z.; Kang, S. K.; et al. Flexible Transient Optical Waveguides and Surface-Wave Biosensors Constructed from Monocrystalline Silicon. *Adv. Mater.* **2018**, *30*, 1801584.
(162) Kim, D.-H.; Lu, N.; Ma, R.; Kim, Y.-S.; Kim, R.-H.; Wang, S.; Wu, J.; Won, S. M.; Tao, H.; Islam, A.; et al. Epidermal Electronics. *Science* **2011**, *333*, 838−843.
(163) Ko, H. C.; Stoykovich, M. P.; Song, J.; Malyarchuk, V.; Choi, W. M.; Yu, C.-J.; Geddes, J. B., III; Xiao, J.; Wang, S.; Huang, Y.; Rogers, J. A. A Hemispherical Electronic Eye Camera Based on Compressible Silicon Optoelectronics. *Nature* **2008**, *454*, 748−753.
(164) Zhang, C.; Chen, J.; Gao, J.; Tan, G.; Bai, S.; Weng, K.; Chen, H. M.; Ding, X.; Cheng, H.; Yang, Y.; Wang, J. Laser Processing of Crumpled Porous Graphene/Mxene Nanocomposites for a Stand-alone Gas Sensing System. *Nano Lett.* **2023**, *23*, 3435−3443.
(165) Wang, Y.; Qiu, L.; Luo, Y.; Ding, R. A Stretchable and Large-Scale Guided Wave Sensor Network for Aircraft Smart Skin of Structural Health Monitoring. *Struct. Health Monit.* **2021**, *20*, 861−876.
(166) Yun, J.; Lim, Y.; Jang, G. N.; Kim, D.; Lee, S.-J.; Park, H.; Hong, S. Y.; Lee, G.; Zi, G.; Ha, J. S. Stretchable Patterned Graphene Gas Sensor Driven by Integrated Micro-Supercapacitor Array. *Nano Energy* **2016**, *19*, 401−414.
(167) Kim, D.; Kim, D.; Lee, H.; Jeong, Y. R.; Lee, S. J.; Yang, G.; Kim, H.; Lee, G.; Jeon, S.; Zi, G.; et al. Body-Attachable and Stretchable Multisensors Integrated with Wirelessly Rechargeable Energy Storage Devices. *Adv. Mater.* **2016**, *28*, 748−756.
(168) Jiang, Y.; Zhang, Z.; Wang, Y.-X.; Li, D.; Coen, C.-T.; Hwaun, E.; Chen, G.; Wu, H.-C.; Zhong, D.; Niu, S.; et al. Topological Supramolecular Network Enabled High-Conductivity, Stretchable Organic Bioelectronics. *Science* **2022**, *375*, 1411−1417.
(169) Kim, D.; Min, J.; Ko, S. H. Recent Developments and Future Directions of Wearable Skin Biosignal Sensors. *Adv. Sens. Res.* **2023**, 2300118.
(170) Kim, M.; Lim, H.; Ko, S. H. Liquid Metal Patterning and Unique Properties for Next-Generation Soft Electronics. *Adv. Sci.* **2023**, *10*, 2205795.
(171) Choi, J.; Min, J.; Kim, D.; Kim, J.; Kim, J.; Yoon, H.; Lee, J.; Jeong, Y.; Kim, C.-Y.; Ko, S. H. Hierarchical 3d Percolation Network of Ag-Au Core-Shell Nanowire-Hydrogel Composite for Efficient Biohybride Electrodes. *ACS Nano* **2023**, *17*, 17966−17978.
(172) Kim, K. K.; Kim, M.; Pyun, K.; Kim, J.; Min, J.; Koh, S.; Root, S. E.; Kim, J.; Nguyen, B.-N. T.; Nishio, Y. A Substrate-Less Nanomesh Receptor with Meta-Learning for Rapid Hand Task Recognition. *Nat. Electron.* **2023**, *6*, 64−75.
(173) Hong, I.; Lee, S.; Kim, D.; Cho, H.; Roh, Y.; An, H.; Hong, S.; Ko, S. H.; Han, S. Study on the Oxidation of Copper Nanowire Network Electrodes for Skin Mountable Flexible, Stretchable and Wearable Electronics Applications. *Nanotechnology* **2019**, *30*, 074001.
(174) Won, P.; Coyle, S.; Ko, S. H.; Quinn, D.; Hsia, K. J.; LeDuc, P.; Majidi, C. Controlling C2c12 Cytotoxicity on Liquid Metal Embedded Elastomer (Lmee). *Adv. Healthcare Mater.* **2023**, *12*, 2202430.
(175) Kim, M.; Park, J. J.; Cho, C.; Ko, S. H. Liquid Metal Based Stretchable Room Temperature Soldering Sticker Patch for Stretchable Electronics Integration. *Adv. Funct. Mater.* **2023**, *33*, 2303286.
(176) Ashammakhi, N.; Hernandez, A. L.; Unluturk, B. D.; Quintero, S. A.; de Barros, N. R.; Hoque Apu, E.; Bin Shams, A.; Ostrovidov, S.; Li, J.; Contag, C.; et al. Biodegradable Implantable Sensors: Materials Design, Fabrication, and Applications. *Adv. Funct. Mater.* **2021**, *31*, 2104149.
(177) Zaaba, N. F.; Jaafar, M. A Review on Degradation Mechanisms of Polylactic Acid: Hydrolytic, Photodegradative, Microbial, and Enzymatic Degradation. *Polym. Eng. Sci.* **2020**, *60*, 2061−2075.
(178) Vert, M.; Doi, Y.; Hellwich, K.-H.; Hess, M.; Hodge, P.; Kubisa, P.; Rinaudo, M.; Schué, F. Terminology for Biorelated Polymers and Applications (Iupac Recommendations 2012). *Pure Appl. Chem.* **2012**, *84*, 377−410.
(179) Xie, F.; Zhang, T.; Bryant, P.; Kurusingal, V.; Colwell, J. M.; Laycock, B. Degradation and Stabilization of Polyurethane Elastomers. *Prog. Polym. Sci.* **2019**, *90*, 211−268.
(180) Iglesias-Montes, M. L.; Soccio, M.; Luzi, F.; Puglia, D.; Gazzano, M.; Lotti, N.; Manfredi, L. B.; Cyras, V. P. Evaluation of the Factors Affecting the Disintegration under a Composting Process of Poly (Lactic Acid)/Poly (3-Hydroxybutyrate)(Pla/Phb) Blends. *Polymers* **2021**, *13*, 3171.

https://doi.org/10.1021/acsnano.3c11832
ACS Nano 2024, 18, 3969−3995

(181) De Santis, M.; Cacciotti, I. Wireless Implantable and Biodegradable Sensors for Postsurgery Monitoring: Current Status and Future Perspectives. *Nanotechnology* **2020**, *31*, 252001.
(182) Cheng, H.; Vepachedu, V. Recent Development of Transient Electronics. *Theor. Appl. Mech. Lett.* **2016**, *6*, 21−31.
(183) Choi, Y.; Koo, J.; Rogers, J. A. Inorganic Materials for Transient Electronics in Biomedical Applications. *MRS Bull.* **2020**, *45*, 103−112.
(184) Yin, L.; Cheng, H.; Mao, S.; Haasch, R.; Liu, Y.; Xie, X.; Hwang, S. W.; Jain, H.; Kang, S. K.; Su, Y.; et al. Dissolvable Metals for Transient Electronics. *Adv. Funct. Mater.* **2014**, *24*, 645−658.
(185) Kang, S.-K.; Park, G.; Kim, K.; Hwang, S.-W.; Cheng, H.; Shin, J.; Chung, S.; Kim, M.; Yin, L.; Lee, J. C.; et al. Dissolution Chemistry and Biocompatibility of Silicon-and Germanium-Based Semiconductors for Transient Electronics. *ACS Appl. Mater. Interfaces* **2015**, *7*, 9297−9305.
(186) Kang, S.-K.; Murphy, R. K.; Hwang, S.-W.; Lee, S. M.; Harburg, D. V.; Krueger, N. A.; Shin, J.; Gamble, P.; Cheng, H.; Yu, S.; et al. Bioresorbable Silicon Electronic Sensors for the Brain. *Nature* **2016**, *530*, 71−76.
(187) Zhao, H.; Xue, Z.; Wu, X.; Wei, Z.; Guo, Q.; Xu, M.; Qu, C.; You, C.; Mei, Y.; Zhang, M.; et al. Biodegradable Germanium Electronics for Integrated Biosensing of Physiological Signals. *npj Flexible Electron.* **2022**, *6*, 63.
(188) Lu, D.; Liu, T. L.; Chang, J. K.; Peng, D.; Zhang, Y.; Shin, J.; Hang, T.; Bai, W.; Yang, Q.; Rogers, J. A. Transient Light-Emitting Diodes Constructed from Semiconductors and Transparent Conductors That Biodegrade under Physiological Conditions. *Adv. Mater.* **2019**, *31*, 1902739.
(189) Kang, S. K.; Hwang, S. W.; Cheng, H.; Yu, S.; Kim, B. H.; Kim, J. H.; Huang, Y.; Rogers, J. A. Dissolution Behaviors and Applications of Silicon Oxides and Nitrides in Transient Electronics. *Adv. Funct. Mater.* **2014**, *24*, 4427−4434.
(190) Corsi, M.; Paghi, A.; Mariani, S.; Golinelli, G.; Debrassi, A.; Egri, G.; Leo, G.; Vandini, E.; Vilella, A.; Dahne, L. Implantable and Bioresorbable Nanostructured Fluorescence Sensor for In Vivo pH Monitoring. In *2022 IEEE Sensors*; IEEE, 2022; pp 1−4.
(191) Lu, D.; Yan, Y.; Deng, Y.; Yang, Q.; Zhao, J.; Seo, M.-H.; Bai, W.; MacEwan, M. R.; Huang, Y.; Ray, W. Z.; Rogers, J. A. Bioresorbable Wireless Sensors as Temporary Implants for in Vivo Measurements of Pressure. *Adv. Funct. Mater.* **2020**, *30*, 2003754.
(192) Ko, G.-J.; Han, S. D.; Kim, J.-K.; Zhu, J.; Han, W. B.; Chung, J.; Yang, S. M.; Cheng, H.; Kim, D.-H.; Kang, C.-Y.; Hwang, S.-W. Biodegradable, Flexible Silicon Nanomembrane-Based Nox Gas Sensor System with Record-High Performance for Transient Environmental Monitors and Medical Implants. *NPG Asia Mater.* **2020**, *12*, 71.
(193) Falcucci, T.; Presley, K. F.; Choi, J.; Fizpatrick, V.; Barry, J.; Kishore Sahoo, J.; Ly, J. T.; Grusenmeyer, T. A.; Dalton, M. J.; Kaplan, D. L. Degradable Silk-Based Subcutaneous Oxygen Sensors. *Adv. Funct. Mater.* **2022**, *32*, 2202020.
(194) Han, H.-S.; Loffredo, S.; Jun, I.; Edwards, J.; Kim, Y.-C.; Seok, H.-K.; Witte, F.; Mantovani, D.; Glyn-Jones, S. Current Status and Outlook on the Clinical Translation of Biodegradable Metals. *Mater. Today* **2019**, *23*, 57−71.
(195) Li, Y.; Chen, W.; Lu, L. Wearable and Biodegradable Sensors for Human Health Monitoring. *ACS Appl. Bio Mater.* **2021**, *4*, 122−139.
(196) Fu, K. K.; Wang, Z.; Dai, J.; Carter, M.; Hu, L. Transient Electronics: Materials and Devices. *Chem. Mater.* **2016**, *28*, 3527−3539.
(197) Redlich, C.; Schauer, A.; Scheibler, J.; Poehle, G.; Barthel, P.; Maennel, A.; Adams, V.; Weissgaerber, T.; Linke, A.; Quadbeck, P. In Vitro Degradation Behavior and Biocompatibility of Bioresorbable Molybdenum. *Metals* **2021**, *11*, 761.
(198) Sezer, N.; Evis, Z.; Kayhan, S. M.; Tahmasebifar, A.; Koç, M. Review of Magnesium-Based Biomaterials and Their Applications. *J. Magnesium Alloys* **2018**, *6*, 23−43.
(199) Lee, Y. K.; Yu, K. J.; Song, E.; Barati Farimani, A.; Vitale, F.; Xie, Z.; Yoon, Y.; Kim, Y.; Richardson, A.; Luan, H.; et al. Dissolution of Monocrystalline Silicon Nanomembranes and Their Use as Encapsulation Layers and Electrical Interfaces in Water-Soluble Electronics. *ACS Nano* **2017**, *11*, 12562−12572.
(200) Wang, L.; Gao, Y.; Dai, F.; Kong, D.; Wang, H.; Sun, P.; Shi, Z.; Sheng, X.; Xu, B.; Yin, L. Geometrical and Chemical-Dependent Hydrolysis Mechanisms of Silicon Nanomembranes for Biodegradable Electronics. *ACS Appl. Mater. Interfaces* **2019**, *11*, 18013−18023.
(201) Li, R.; Wang, L.; Yin, L. Materials and Devices for Biodegradable and Soft Biomedical Electronics. *Materials* **2018**, *11*, 2108.
(202) Kim, D.-H.; Kim, Y.-S.; Amsden, J.; Panilaitis, B.; Kaplan, D. L.; Omenetto, F. G.; Zakin, M. R.; Rogers, J. A. Silicon Electronics on Silk as a Path to Bioresorbable, Implantable Devices. *Appl. Phys. Lett.* **2009**, *95*, 133701.
(203) Lee, W. H.; Cha, G. D.; Kim, D.-H. Flexible and Biodegradable Electronic Implants for Diagnosis and Treatment of Brain Diseases. *Curr. Opin. Biotechnol.* **2021**, *72*, 13−21.
(204) Chang, J.-K.; Fang, H.; Bower, C. A.; Song, E.; Yu, X.; Rogers, J. A. Materials and Processing Approaches for Foundry-Compatible Transient Electronics. *Proc. Natl. Acad. Sci. U. S. A.* **2017**, *114*, No. E5522.
(205) La Mattina, A. A.; Mariani, S.; Barillaro, G. Bioresorbable Materials on the Rise: From Electronic Components and Physical Sensors to in Vivo Monitoring Systems. *Adv. Sci.* **2020**, *7*, 1902872.
(206) Teo, B. K.; Sun, X. H. Silicon-Based Low-Dimensional Nanomaterials and Nanodevices. *Chem. Rev.* **2007**, *107*, 1454−1532.
(207) Huang, X. Materials and Applications of Bioresorbable Electronics. *J. Semicond.* **2018**, *39*, 011003.
(208) Kang, S. K.; Hwang, S. W.; Yu, S.; Seo, J. H.; Corbin, E. A.; Shin, J.; Wie, D. S.; Bashir, R.; Ma, Z.; Rogers, J. A. Biodegradable Thin Metal Foils and Spin-on Glass Materials for Transient Electronics. *Adv. Funct. Mater.* **2015**, *25*, 1789−1797.
(209) Yu, X.; Shou, W.; Mahajan, B. K.; Huang, X.; Pan, H. Materials, Processes, and Facile Manufacturing for Bioresorbable Electronics: A Review. *Adv. Mater.* **2018**, *30*, 1707624.
(210) Gewert, B.; Plassmann, M. M.; MacLeod, M. Pathways for Degradation of Plastic Polymers Floating in the Marine Environment. *Environ. Sci. Processes Impacts* **2015**, *17*, 1513−1521.
(211) Hosseini, E. S.; Dervin, S.; Ganguly, P.; Dahiya, R. Biodegradable Materials for Sustainable Health Monitoring Devices. *ACS Appl. Bio Mater.* **2021**, *4*, 163−194.
(212) Jiang, W.; Li, H.; Liu, Z.; Li, Z.; Tian, J.; Shi, B.; Zou, Y.; Ouyang, H.; Zhao, C.; Zhao, L.; et al. Fully Bioabsorbable Natural-Materials-Based Triboelectric Nanogenerators. *Adv. Mater.* **2018**, *30*, 1801895.
(213) Zhu, B.; Wang, H.; Leow, W. R.; Cai, Y.; Loh, X. J.; Han, M. Y.; Chen, X. Silk Fibroin for Flexible Electronic Devices. *Adv. Mater.* **2016**, *28*, 4250−4265.
(214) Jung, Y. H.; Chang, T.-H.; Zhang, H.; Yao, C.; Zheng, Q.; Yang, V. W.; Mi, H.; Kim, M.; Cho, S. J.; Park, D.-W.; et al. High-Performance Green Flexible Electronics Based on Biodegradable Cellulose Nanofibril Paper. *Nat. Commun.* **2015**, *6*, 7170.
(215) Wang, H.; Zhu, B.; Ma, X.; Hao, Y.; Chen, X. Physically Transient Resistive Switching Memory Based on Silk Protein. *Small* **2016**, *12*, 2715−2719.
(216) Middleton, J. C.; Tipton, A. J. Synthetic Biodegradable Polymers as Orthopedic Devices. *Biomaterials* **2000**, *21*, 2335−2346.
(217) Hwang, S. W.; Song, J. K.; Huang, X.; Cheng, H.; Kang, S. K.; Kim, B. H.; Kim, J. H.; Yu, S.; Huang, Y.; Rogers, J. A. High-Performance Biodegradable/Transient Electronics on Biodegradable Polymers. *Adv. Mater.* **2014**, *26*, 3905−3911.
(218) Reddy, M. S. B.; Ponnamma, D.; Choudhary, R.; Sadasivuni, K. K. A Comparative Review of Natural and Synthetic Biopolymer Composite Scaffolds. *Polymers* **2021**, *13*, 1105.
(219) Yoon, J.; Han, J.; Choi, B.; Lee, Y.; Kim, Y.; Park, J.; Lim, M.; Kang, M.-H.; Kim, D. H.; Kim, D. M.; et al. Three-Dimensional Printed Poly (Vinyl Alcohol) Substrate with Controlled on-Demand

Degradation for Transient Electronics. *ACS Nano* **2018**, *12*, 6006−6012.
(220) Kumar, R.; Ranwa, S.; Kumar, G. Biodegradable Flexible Substrate Based on Chitosan/Pvp Blend Polymer for Disposable Electronics Device Applications. *J. Phys. Chem. B* **2020**, *124*, 149−155.
(221) Llorens, E.; Armelin, E.; del Mar Pérez-Madrigal, M.; Del Valle, L. J.; Alemán, C.; Puiggalí, J. Nanomembranes and Nanofibers from Biodegradable Conducting Polymers. *Polymers* **2013**, *5*, 1115−1157.
(222) Brannigan, R. P.; Dove, A. P. Synthesis, Properties and Biomedical Applications of Hydrolytically Degradable Materials Based on Aliphatic Polyesters and Polycarbonates. *Biomater. Sci.* **2017**, *5*, 9−21.
(223) Nair, L. S.; Laurencin, C. T. Biodegradable Polymers as Biomaterials. *Prog. Polym. Sci.* **2007**, *32*, 762−798.
(224) Feig, V. R.; Tran, H.; Bao, Z. Biodegradable Polymeric Materials in Degradable Electronic Devices. *ACS Cent. Sci.* **2018**, *4*, 337−348.
(225) Frost, M. C.; Meyerhoff, M. E. Implantable Chemical Sensors for Real-Time Clinical Monitoring: Progress and Challenges. *Curr. Opin. Chem. Biol.* **2002**, *6*, 633−641.
(226) Manjakkal, L.; Dervin, S.; Dahiya, R. Flexible Potentiometric Ph Sensors for Wearable Systems. *RSC Adv.* **2020**, *10*, 8594−8617.
(227) Dang, W.; Manjakkal, L.; Navaraj, W. T.; Lorenzelli, L.; Vinciguerra, V.; Dahiya, R. Stretchable Wireless System for Sweat Ph Monitoring. *Biosens. Bioelectron.* **2018**, *107*, 192−202.
(228) Ling, W.; Yu, J.; Ma, N.; Li, Y.; Wu, Z.; Liang, R.; Hao, Y.; Pan, H.; Liu, W.; Fu, B.; et al. Flexible Electronics and Materials for Synchronized Stimulation and Monitoring in Multi-Encephalic Regions. *Adv. Funct. Mater.* **2020**, *30*, 2002644.
(229) Yang, H.; Qian, Z.; Wang, J.; Feng, J.; Tang, C.; Wang, L.; Guo, Y.; Liu, Z.; Yang, Y.; Zhang, K.; et al. Carbon Nanotube Array-Based Flexible Multifunctional Electrodes to Record Electrophysiology and Ions on the Cerebral Cortex in Real Time. *Adv. Funct. Mater.* **2022**, *32*, 2204794.
(230) Li, J.; Liu, Y.; Yuan, L.; Zhang, B.; Bishop, E. S.; Wang, K.; Tang, J.; Zheng, Y.-Q.; Xu, W.; Niu, S. A Tissue-Like Neurotransmitter Sensor for the Brain and Gut. *Nature* **2022**, *606*, 94−101.
(231) Xie, K.; Wang, N.; Lin, X.; Wang, Z.; Zhao, X.; Fang, P.; Yue, H.; Kim, J.; Luo, J.; Cui, S.; et al. Organic Electrochemical Transistor Arrays for Real-Time Mapping of Evoked Neurotransmitter Release in Vivo. *Elife* **2020**, *9*, No. e50345.
(232) Wang, L.; Xie, S.; Wang, Z.; Liu, F.; Yang, Y.; Tang, C.; Wu, X.; Liu, P.; Li, Y.; Saiyin, H.; et al. Functionalized Helical Fibre Bundles of Carbon Nanotubes as Electrochemical Sensors for Long-Term in Vivo Monitoring of Multiple Disease Biomarkers. *Nat. Biomed. Eng.* **2020**, *4*, 159−171.
(233) Li, Q.; Li, D.; Lu, J.; Zou, K.; Wang, L.; Jiao, Y.; Wang, M.; Gao, R.; Song, J.; Li, Y.; et al. Interface-Stabilized Fiber Sensor for Real-Time Monitoring of Amniotic Fluid During Pregnancy. *Adv. Mater.* **2023**, 2307726.
(234) Deng, Y.; Qi, H.; Ma, Y.; Liu, S.; Zhao, M.; Guo, Z.; Jie, Y.; Zheng, R.; Jing, J.; Chen, K.; et al. A Flexible and Highly Sensitive Organic Electrochemical Transistor-Based Biosensor for Continuous and Wireless Nitric Oxide Detection. *Proc. Natl. Acad. Sci. U. S. A.* **2022**, *119*, No. e2208060119.
(235) Li, J.; Li, D.; Yuan, R.; Xiang, Y. Biodegradable Mno2 Nanosheet-Mediated Signal Amplification in Living Cells Enables Sensitive Detection of Down-Regulated Intracellular Microrna. *ACS Appl. Mater. Interfaces* **2017**, *9*, 5717−5724.
(236) Yeo, D.; Wiraja, C.; Chuah, Y. J.; Gao, Y.; Xu, C. A Nanoparticle-Based Sensor Platform for Cell Tracking and Status/Function Assessment. *Sci. Rep.* **2015**, *5*, 14768.
(237) Kraft, M. D.; Btaiche, I. F.; Sacks, G. S.; Kudsk, K. A. Treatment of Electrolyte Disorders in Adult Patients in the Intensive Care Unit. *Am. J. Health. Syst. Pharm.* **2005**, *62*, 1663−1682.
(238) Bakker, E.; Telting-Diaz, M. Electrochemical Sensors. *Anal. Chem.* **2002**, *74*, 2781−2800.
(239) Jimenez de Aberasturi, D.; Montenegro, J.-M.; Ruiz de Larramendi, I.; Rojo, T.; Klar, T. A.; Alvarez-Puebla, R.; Liz-Marzán, L. M.; Parak, W. J. Optical Sensing of Small Ions with Colloidal Nanoparticles. *Chem. Mater.* **2012**, *24*, 738−745.
(240) Dienel, G. A.; Cruz, N. F. Aerobic Glycolysis During Brain Activation: Adrenergic Regulation and Influence of Norepinephrine on Astrocytic Metabolism. *Journal of neurochemistry* **2016**, *138*, 14−52.
(241) Förstermann, U.; Sessa, W. C. Nitric Oxide Synthases: Regulation and Function. *Eur. Heart J.* **2012**, *33*, 829−837.
(242) Steinhorn, B. S.; Loscalzo, J.; Michel, T. Nitroglycerin and Nitric Oxide-a Rondo of Themes in Cardiovascular Therapeutics. *N. Engl. J. Med.* **2015**, *373*, 277−280.
(243) Flynn, C. D.; Chang, D.; Mahmud, A.; Yousefi, H.; Das, J.; Riordan, K. T.; Sargent, E. H.; Kelley, S. O. Biomolecular Sensors for Advanced Physiological Monitoring. *Nat. Rev. Bioeng.* **2023**, *1*, 560.
(244) Liu, H.; Yang, A.; Song, J.; Wang, N.; Lam, P.; Li, Y.; Law, H. K.-w.; Yan, F. Ultrafast, Sensitive, and Portable Detection of Covid-19 Igg Using Flexible Organic Electrochemical Transistors. *Sci. Adv.* **2021**, *7*, No. eabg8387.
(245) Tu, J.; Min, J.; Song, Y.; Xu, C.; Li, J.; Moore, J.; Hanson, J.; Hu, E.; Parimon, T.; Wang, T.-Y.; et al. A Wireless Patch for the Monitoring of C-Reactive Protein in Sweat. *Nat. Biomed. Eng.* **2023**, *7*, 1293.
(246) Dong, H.; Lei, J.; Ding, L.; Wen, Y.; Ju, H.; Zhang, X. Microrna: Function, Detection, and Bioanalysis. *Chem. Rev.* **2013**, *113*, 6207−6233.
(247) Morales, M. A.; Halpern, J. M. Guide to Selecting a Biorecognition Element for Biosensors. *Bioconjugate Chem.* **2018**, *29*, 3231−3239.
(248) Yi, J.; Zou, G.; Huang, J.; Ren, X.; Tian, Q.; Yu, Q.; Wang, P.; Yuan, Y.; Tang, W.; Wang, C.; et al. Water-Responsive Supercontractile Polymer Films for Bioelectronic Interfaces. *Nature* **2023**, *624*, 295−302.
(249) Xu, J.; Wang, S.; Wang, G.-J. N.; Zhu, C.; Luo, S.; Jin, L.; Gu, X.; Chen, S.; Feig, V. R.; To, J. W.; et al. Highly Stretchable Polymer Semiconductor Films through the Nanoconfinement Effect. *Science* **2017**, *355*, 59−64.
(250) Zhuang, Q.; Yao, K.; Wu, M.; Lei, Z.; Chen, F.; Li, J.; Mei, Q.; Zhou, Y.; Huang, Q.; Zhao, X.; et al. Wafer-Patterned, Permeable, and Stretchable Liquid Metal Microelectrodes for Implantable Bioelectronics with Chronic Biocompatibility. *Sci. Adv.* **2023**, *9*, No. eadg8602.
(251) Yuk, H.; Wu, J.; Zhao, X. Hydrogel Interfaces for Merging Humans and Machines. *Nat. Rev. Mater.* **2022**, *7*, 935−952.
(252) Salatino, J. W.; Ludwig, K. A.; Kozai, T. D.; Purcell, E. K. Glial Responses to Implanted Electrodes in the Brain. *Nat. Biomed. Eng.* **2017**, *1*, 862−877.
(253) Canham, L. Nanoscale Semiconducting Silicon as a Nutritional Food Additive. *Nanotechnology* **2007**, *18*, 185704.
(254) Lin, Y.; Bariya, M.; Nyein, H. Y. Y.; Kivimäki, L.; Uusitalo, S.; Jansson, E.; Ji, W.; Yuan, Z.; Happonen, T.; Liedert, C.; et al. Porous Enzymatic Membrane for Nanotextured Glucose Sweat Sensors with High Stability toward Reliable Noninvasive Health Monitoring. *Adv. Funct. Mater.* **2019**, *29*, 1902521.
(255) Tu, J.; Torrente-Rodríguez, R. M.; Wang, M.; Gao, W. The Era of Digital Health: A Review of Portable and Wearable Affinity Biosensors. *Adv. Funct. Mater.* **2020**, *30*, 1906713.
(256) Lee, G.; Choi, Y. S.; Yoon, H.-J.; Rogers, J. A. Advances in Physicochemically Stimuli-Responsive Materials for on-Demand Transient Electronic Systems. *Matter* **2020**, *3*, 1031−1052.
(257) Liu, G.; Lv, Z.; Batool, S.; Li, M. Z.; Zhao, P.; Guo, L.; Wang, Y.; Zhou, Y.; Han, S. T. Biocompatible Material-Based Flexible Biosensors: From Materials Design to Wearable/Implantable Devices and Integrated Sensing Systems. *Small* **2023**, *19*, 2207879.
(258) Kim, C. Y.; Ku, M. J.; Qazi, R.; Nam, H. J.; Park, J. W.; Nam, K. S.; Oh, S.; Kang, I.; Jang, J.-H.; Kim, W. Y.; et al. Soft Subdermal Implant Capable of Wireless Battery Charging and Programmable

https://doi.org/10.1021/acsnano.3c11832
ACS Nano 2024, 18, 3969−3995

Controls for Applications in Optogenetics. *Nat. Commun.* **2021**, *12*, 535.
(259) Stuart, T.; Cai, L.; Burton, A.; Gutruf, P. Wireless and Battery-Free Platforms for Collection of Biosignals. *Biosens. Bioelectron.* **2021**, *178*, 113007.
(260) Singer, A.; Robinson, J. T. Wireless Power Delivery Techniques for Miniature Implantable Bioelectronics. *Adv. Healthcare Mater.* **2021**, *10*, 2100664.
(261) Lu, L.; Gutruf, P.; Xia, L.; Bhatti, D. L.; Wang, X.; Vazquez-Guardado, A.; Ning, X.; Shen, X.; Sang, T.; Ma, R.; et al. Wireless Optoelectronic Photometers for Monitoring Neuronal Dynamics in the Deep Brain. *Proc. Natl. Acad. Sci. U. S. A.* **2018**, *115*, No. E1374.
(262) Won, S. M.; Cai, L.; Gutruf, P.; Rogers, J. A. Wireless and Battery-Free Technologies for Neuroengineering. *Nat. Biomed. Eng.* **2023**, *7*, 405−423.
(263) Park, S. I.; Brenner, D. S.; Shin, G.; Morgan, C. D.; Copits, B. A.; Chung, H. U.; Pullen, M. Y.; Noh, K. N.; Davidson, S.; Oh, S. J.; et al. Soft, Stretchable, Fully Implantable Miniaturized Optoelectronic Systems for Wireless Optogenetics. *Nat. Biotechnol.* **2015**, *33*, 1280−1286.
(264) Piech, D. K.; Johnson, B. C.; Shen, K.; Ghanbari, M. M.; Li, K. Y.; Neely, R. M.; Kay, J. E.; Carmena, J. M.; Maharbiz, M. M.; Muller, R. A Wireless Millimetre-Scale Implantable Neural Stimulator with Ultrasonically Powered Bidirectional Communication. *Nat. Biomed. Eng.* **2020**, *4*, 207−222.
(265) Chen, J. C.; Kan, P.; Yu, Z.; Alrashdan, F.; Garcia, R.; Singer, A.; Lai, C. E.; Avants, B.; Crosby, S.; Li, Z.; et al. A Wireless Millimetric Magnetoelectric Implant for the Endovascular Stimulation of Peripheral Nerves. *Nat. Biomed. Eng.* **2022**, *6*, 706−716.
(266) Koo, J.; MacEwan, M. R.; Kang, S.-K.; Won, S. M.; Stephen, M.; Gamble, P.; Xie, Z.; Yan, Y.; Chen, Y.-Y.; Shin, J.; et al. Wireless Bioresorbable Electronic System Enables Sustained Nonpharmacological Neuroregenerative Therapy. *Nat. Med.* **2018**, *24*, 1830−1836.
(267) Wang, L.; Lu, C.; Yang, S.; Sun, P.; Wang, Y.; Guan, Y.; Liu, S.; Cheng, D.; Meng, H.; Wang, Q.; et al. A Fully Biodegradable and Self-Electrified Device for Neuroregenerative Medicine. *Sci. Adv.* **2020**, *6*, No. eabc6686.
(268) Sheng, H.; Jiang, L.; Wang, Q.; Zhang, Z.; Lv, Y.; Ma, H.; Bi, H.; Yuan, J.; Shao, M.; Li, F.; et al. A Soft Implantable Energy Supply System That Integrates Wireless Charging and Biodegradable Zn-Ion Hybrid Supercapacitors. *Sci. Adv.* **2023**, *9*, No. eadh8083.
(269) Scholten, K.; Meng, E. A Review of Implantable Biosensors for Closed-Loop Glucose Control and Other Drug Delivery Applications. *Int. J. Pharm.* **2018**, *544*, 319−334.
(270) Saunders, A.; Messer, L. H.; Forlenza, G. P. Minimed 670g Hybrid Closed Loop Artificial Pancreas System for the Treatment of Type 1 Diabetes Mellitus: Overview of Its Safety and Efficacy. *Expert Rev. Med. Devices* **2019**, *16*, 845−853.

https://doi.org/10.1021/acsnano.3c11832
ACS Nano 2024, 18, 3969−3995